NASA MEMO 3-3-59A

NASA MEMO 3-3-59A

NASA MEMORANDUM

SUBSONIC AERODYNAMIC CHARACTERISTICS OF AN AIRPLANE CONFIGURATION WITH A 63° SWEPTBACK WING AND TWIN-BOOM TAILS

By Howard F. Savage and George G. Edwards

Ames Research Center
Moffett Field, Calif.

NATIONAL AERONAUTICS AND SPACE ADMINISTRATION

WASHINGTON
March 1959

[redacted]

NATIONAL AERONAUTICS AND SPACE ADMINISTRATION

MEMORANDUM 3-3-59A

SUBSONIC AERODYNAMIC CHARACTERISTICS OF AN AIRPLANE CONFIGURATION WITH A 63° SWEPTBACK WING AND TWIN-BOOM TAILS*

By Howard F. Savage and George G. Edwards

SUMMARY

A wind-tunnel investigation has been conducted to determine the effects of an unconventional tail arrangement on the subsonic static longitudinal and lateral stability characteristics of a model having a 63° sweptback wing of aspect ratio 3.5 and a fuselage. Tail booms, extending rearward from approximately the midsemispan of each wing panel, supported independent tail assemblies well outboard of the usual position at the rear of the fuselage. The horizontal-tail surfaces had the leading edge swept back 45° and an aspect ratio of 2.4. The vertical tail surfaces were geometrically similar to one panel of the horizontal tail. For comparative purposes, the wing-body combination was also tested with conventional fuselage-mounted tail surfaces. The wind-tunnel tests were conducted at Mach numbers from 0.25 to 0.95 with a Reynolds number of 2,000,000, at a Mach number of 0.46 with a Reynolds number of 3,500,000, and at a Mach number of 0.20 with a Reynolds number of 7,000,000.

The results of the investigation indicate that longitudinal stability existed to considerably higher lift coefficients for the outboard tail configuration than for the configuration with conventional tail. Wing fences were necessary with both configurations for the elimination of sudden changes in longitudinal stability at lift coefficients between 0.3 and 0.5. Sideslip angles up to 15° had only small effects upon the pitching-moment characteristics of the outboard tail configuration. There was an increase in the directional stability for the outboard tail configuration at the higher angles of attack as opposed to a decrease for the conventional tail configuration at most of the Mach numbers and Reynolds numbers of this investigation. The dihedral effect increased rapidly with increasing angle of attack for both the outboard and the conventional tail configurations but the increase was greater for the outboard tail configuration. The data indicate that the outboard tail is an effective roll control.

*Title, Unclassified

[redacted]

[redacted]

INTRODUCTION

The investigation of reference 1 demonstrated that the static longitudinal stability characteristics of an airplane configuration having a 45° sweptback wing of aspect ratio 6 can be markedly improved by the use of horizontal-tail surfaces located well outboard of the usual position at the rear of the fuselage. The outboard tails were mounted on booms extending rearward from about the midsemispan of the wing. Results indicated that the increased effectiveness of the outboard tails over that of the conventional tail in promoting static longitudinal stability at high angles of attack was due to the more favorable downwash field behind the outer portions of the sweptback wing. The wing was, of course, one suitable primarily for subsonic cruise conditions.

The present investigation was undertaken for the purpose of assessing the characteristics of an outboard tail configuration which, by virtue of extreme sweepback of the wing, might be suitable for operation at supersonic speeds. The wing had 63° sweepback of the leading edge and an aspect ratio of 3.5 and from previous investigations was known to have serious pitch-up difficulties at subsonic speeds. In the investigation of reference 2 this wing was tested in combination with a fuselage and conventional fuselage-mounted tail surfaces. It was found that with wing fences of height twice the maximum thickness of the wing, the trend toward longitudinal instability was delayed to higher lift coefficients. There was, however, a serious loss in lift-drag ratio due to the large fences.

In the present investigation the 63° sweptback wing was mounted on a fuselage suitable for the testing with a conventional tail to provide data for direct comparison with data for the outboard tail configuration. The outboard horizontal- and vertical-tail surfaces were mounted on booms extending rearward from either the 40-percent or 50-percent spanwise station of the wing. The tail booms were kept to minimum size consistent with model strength requirements in order that the volume of the configuration be comparable with the one utilizing a conventional tail. Practically, the volume required for storage could be more evenly distributed between the fuselage and the tail booms, resulting in a three-body arrangement of the type suggested in reference 3.

Static longitudinal and lateral stability characteristics were measured for Mach numbers up to 0.95, principally at a Reynolds number of 2,000,000. Several sizes of outboard tails were tested on booms of two different lengths. The effects of wing fences, and extended split flaps, and spoilers were also studied.

[redacted]

NOTATION

All data coefficients are given for the stability system of axes with the origins or moment centers as indicated in table I. The coefficients and symbols are defined as follows:

a	mean-line designation, fraction of chord over which design load is uniform
a_t	lift-curve slope of the isolated horizontal tail, per deg
a_{w+f+t}	lift-curve slope of the wing-fuselage-tail combination, per deg
b	wing span perpendicular to the plane of symmetry
c	local chord parallel to the plane of symmetry
$\bar{c}$	mean aerodynamic chord, ft
C_D	drag coefficient, $\frac{\text{drag}}{qS_w}$
C_l	rolling-moment coefficient, $\frac{\text{rolling moment}}{qS_w b_w}$
C_L	lift coefficient, $\frac{\text{lift}}{qS_w}$
C_m	pitching-moment coefficient, $\frac{\text{pitching moment}}{qS_w \bar{c}_w}$
C_n	yawing-moment coefficient, $\frac{\text{yawing moment}}{qS_w b_w}$
C_Y	lateral-force coefficient, $\frac{\text{lateral force}}{qS_w}$
i_t	incidence of the horizontal tail with respect to the root chord of the wing
l	tail length, longitudinal distance between $\frac{\bar{c}}{4}$ of the tail surface and the moment center of the model
M	free-stream Mach number

[redacted]

p	rolling velocity, radians/sec
q	free-stream dynamic pressure
R	Reynolds number based on the mean aerodynamic chord of the wing
S	area
V	free-stream velocity, ft/sec
$\overline{V}_t$	horizontal-tail volume coefficient, $\frac{S_t l_t}{S_w \bar{c}_w}$
$\overline{V}_v$	vertical-tail volume coefficient, $\frac{S_v l_v}{S_w b_w}$
y	lateral distance from the plane of symmetry
α	angle of attack of the wing root chord, deg
β	angle of sideslip of the body longitudinal axis, deg
ϵ	effective average downwash angle, deg
$\frac{\eta_t q_t}{q}$	tail effectiveness factor (ratio of the lift-curve slope of the horizontal tail in the presence of the wing and the fuselage to the lift-curve slope of the isolated horizontal tail)

Subscripts

w	wing
f	fuselage
t	horizontal tail
v	vertical tail

MODEL

Photographs of the model mounted in the Ames 12-foot pressure wind tunnel are presented in figure 1 and dimensions of the model are given in figure 2 and table II.

[redacted]

The wing-fuselage combination was the same as that used in the investigation of reference 2 except that a shortened version of the fuselage was used in conjunction with the outboard tails. The solid steel wing, which had a leading-edge sweepback of 63°, a taper ratio of 0.25, and an aspect ratio of 3.50, was mounted on the center line of the fuselage. The streamwise airfoil section of the wing had the NACA 64A005 thickness distribution combined with a = 1 mean camber line. The wing was cambered and twisted to provide, theoretically, a uniform distribution of lift over its surface for a lift coefficient of 0.25 at a Mach number of 1.50. The twist and camber distributions are presented in figure 3. Additional details concerning the design of this wing can be found in reference 4. The boundary-layer fences used for some of the tests extended around the leading edge of the wing to 0.15 chord on the lower surface (see fig. 2(b) for fence details). The fence at 0.75 b/2 extended to the trailing edge on the upper surface while the one at 0.30 b/2 extended only over the forward 30 percent of the wing. A fence around the leading edge of the wing at the position of the tail boom was also used in some of the tests.

The outboard horizontal-tail surfaces had a leading-edge sweepback of 45°, a taper ratio of 0.25, and an aspect ratio of 2.40. The outboard vertical-tail surfaces were geometrically similar to one half of the outboard horizontal tails. The streamwise airfoil sections of the outboard tails had the NACA 0004-64 thickness distributions. Horizontal tail surfaces of three sizes were used and are referred to throughout the report as "large," "medium," or "small." The fuselage-mounted tail surfaces used for some of the tests were the same unswept horizontal and sweptback vertical tails of reference 2. Other geometric properties of the tail surfaces are given in figure 2 and table II.

The tail booms were constructed of solid steel and had an elliptical cross section. The major axis was vertical and was twice the minor axis. Booms of two lengths were used to provide for a variation of longitudinal position of the tail surfaces. The booms were attached to the wing at either 0.4 b/2 or 0.5 b/2 (see fig. 4 for sketch of juncture with wing) and were constructed so that the hinge lines (through $\bar{c}_t/4$) of the horizontal tails were in the plane containing the wing leading edges. The gaps between the horizontal tails and the tail booms varied with tail incidence and were left unsealed.

Plain spoilers were simulated by aluminum angle brackets attached to the upper surface of the wing. Spoilers of several heights were provided which could be attached to the upper surface of the wing at 0.07, 0.15, or 0.25 chord (parallel to the plane of symmetry) behind the wing leading edge (see fig. 2(b) for a typical spoiler). The spoilers extended either from the fuselage to 0.50 $b_w/2$, or between 0.21 $b_w/2$ and 0.40 $b_w/2$. The trailing-edge flaps had chords of 0.20 of the wing chord measured

parallel to the plane of symmetry and extended from the fuselage to the tail boom at 0.5 b/2. The simulated hinge lines of the flaps were coincident with the wing trailing edge and the deflection was 31.6° in a plane parallel to the plane of symmetry (fig. 2(b)).

CORRECTIONS TO DATA

Corrections to the data to account for induced tunnel-wall interference originating from lift on the model have been evaluated by the method of reference 5. The corrections showed insignificant variations with Mach number. The following corrections were added:

$$\Delta\alpha = 0.30\ C_L$$

$$\Delta C_D = 0.0045\ C_L^2$$

$$\Delta C_m = 0.003\ C_L$$

The constriction effects of the tunnel walls have been calculated by the method of reference 6. The magnitude of the corrections applied to the Mach number and to the dynamic pressure are illustrated by the following table:

Corrected Mach number	Uncorrected Mach number	$\frac{q_{uncorrected}}{q_{corrected}}$
0.950	0.933	0.982
.900	.892	.990
.800	.797	.995
.600	.599	.997
.460	.459	.998
.200	.200	.998

All the data presented herein were obtained with a 4-inch diameter supporting sting protruding from the rear of the fuselage.

Since for some configurations, the tips of the outboard tails were close to the sting support, tests were conducted to determine whether the size of the sting had any effect on the measured forces. Some data were obtained with both the standard 4-inch sting and with a 2-inch sting. Two configurations, one with outboard tails and the other with a fuselage-mounted tail, were tested at sideslip angles to 12° and at several Mach numbers. There were no significant effects of changing sting size on the force and moment coefficients of either configuration. The main effect of variation of sting size was to alter the pressure at the base of the

model and thus the measured chord force. When the chord force was adjusted to correspond to a base pressure equal to free-stream static pressure, the chord forces were about equal for the two sting sizes investigated. Consequently, all coefficients presented have been corrected to a condition of free-stream static pressure at the base of the model.

TESTS

The initial tests were conducted with varying angle of attack at zero sideslip. Tests were conducted to evaluate the effects of horizontal tail position and size, wing fences, flaps, and spoilers on the longitudinal aerodynamic characteristics of the model. Selected configurations were tested through the range of Mach numbers to 0.95. For one of the better configurations from the standpoint of static longitudinal stability, the incidence of the horizontal tail was varied from -4° to -10° to provide the data necessary for the computation of the effective average downwash. Tests were also conducted with the left horizontal tail set at various incidences to provide data for assessing the lateral-control effectiveness of differential deflection of the horizontal tails.

Tests were conducted with varying α at $\beta \approx 0^\circ$, -6°, -8.35°, and -12°, and with varying β at $\alpha \approx 0^\circ$, 6°, 8.35°, and 12° to evaluate the effects of sideslip angle on the longitudinal and lateral characteristics.

The outboard vertical tails were mounted on the model for all runs made with the tail booms attached to the wing. The conventional vertical tail was installed for all runs with conventional horizontal tail and was removed when the horizontal tail was removed.

RESULTS AND DISCUSSION

Longitudinal Characteristics of Various Configurations at Zero Sideslip

To facilitate comparison of the pitching-moment characteristics of the various configurations, the moment centers were chosen so that all configurations would have about the same static margin at zero lift at a Mach number of 0.20 and a Reynolds number of 7,000,000. Moment centers for the various configurations are given in table I along with the tail lengths and tail volume coefficients.

Effects of tail position.- The variation of pitching-moment coefficient with lift coefficient for the wing-body-tail combination with the medium tail in several positions is presented in figure 4. The

pitching-moment data for the tail-off configuration are also presented. Moving the tail from 0.4 b/2 to 0.5 b/2 improved the pitching-moment characteristics, but there were only small effects due to increasing tail length at either spanwise position. Although the trend toward instability occurred at about the same C_L for either the tail-on or the tail-off configuration, the change in dC_m/dC_L over the lift-coefficient range was considerably less for the tail-on configurations. The over-all favorable effect of moving the outboard tail from 0.4 b/2 to 0.5 b/2 was expected because of a more favorable downwash field at the latter tail position.

Effects of tail size.- The results presented in figure 4 indicate that with the medium tail, a linear pitching-moment curve was not obtained for any of the tail positions investigated. The horizontal tail contribution to the static longitudinal stability is given by the following expression:

$$\left[\left(\frac{dC_m}{dC_L}\right)_{w+f+t}\right] = \frac{-a_t}{a_{w+f+t}} \bar{V}_t \left[\frac{\eta_t q_t}{q}\left(1-\frac{d\epsilon}{d\alpha}\right) + \alpha_t \frac{\partial(\eta_t q_t/q)}{\partial\alpha}\right] \qquad (1)$$

The tail contribution to stability is proportional to $\bar{V}_t$ and thus to tail area. To investigate the effects of changing tail size, outboard horizontal tails having the identical plan form but with areas of 75 and 158 percent of the medium tail were tested in the rearward position at 0.5 b/2 in combination with a full fence at 0.75 b/2 and a leading-edge fence ahead of the tail boom. The pitching-moment data obtained at several Mach numbers and Reynolds numbers are presented in figure 5 for the model with large and medium tails and with no tail; the small tail was tested only at $M = 0.46$, $R = 3{,}500{,}000$. With the moment centers used, the tail volume coefficients, $\bar{V}_t$, were 0.169, 0.226, and 0.347 (see table I). The data of figure 5 show the advantages of increased tail size in reducing longitudinal stability changes at the higher lift coefficients. At Mach numbers of 0.80 and 0.90, good longitudinal stability existed to the limit C_L of the tests for the configuration with large horizontal tails. At a Mach number of 0.46, a loss in longitudinal stability occurred above a C_L of about 0.80. If it is assumed that the tail contribution to stability is directly proportional to $\bar{V}_t$ and that the effective downwash is not affected by changing tail size in a non-uniform downwash field, a simple calculation shows that to maintain the same longitudinal stability at $C_L = 0.90$ as at $C_L = 0$, a tail volume coefficient of 0.49 is required. If it is assumed that the longitudinal position of the moment center is adjusted to maintain the same static margin, the required tail area is 1.55 times the area of the large tail. The effects of increasing tail size were not pursued further.

Effects of fences.- It will be noted in figure 4 that some sudden changes in longitudinal stability occur in the range of lift coefficients from 0.3 to about 0.5. These changes, which occur whether the tail is

on or off, are caused by flow changes on the wing. The wing fence is one means of delaying flow separation to higher lift coefficients and reducing longitudinal stability changes on a swept wing. They would probably seriously impair the efficiency of a supersonic wing, however. Fences were used in this investigation on the assumption that, in some measure at least, the downwash field behind a wing with fences approximates that of a wing without fences with improved twist, camber, and thickness distributions such that the trend toward longitudinal instability is delayed to higher lift coefficients. Figure 6 shows the effects of various wing fences on the pitching-moment characteristics of the configurations with no tail and with tails of three different sizes in the rearward position at spanwise station 0.5 b/2. In general, it may be said that the addition of wing fences improved the pitching-moment characteristics of the model with any of the three tails, the improvement being greater when more fences were used.

Outboard tail configurations compared with conventional tail configurations.- The pitching-moment characteristics of two configurations with large outboard tails and two configurations with conventional tails are compared in figure 7 at several Mach and Reynolds numbers. The outboard tail configurations differed only in tail length, the tails being located at 0.5 b/2 in both cases. The conventional tail configurations differed in tail length and plan form and in fence configurations. The data of figure 7 indicate only small effects of changes in outboard tail length and that, except at $M = 0.20$, both configurations maintain at least neutral stability to higher lift coefficients than either of the conventional tail configurations. It should be emphasized that the conventional tail configuration of reference 2 (see fig. 7) has a tail volume coefficient 1.9 times that of the outboard tail in the forward position. The conventional tail configuration with $\overline{V}_t = 0.308$, which is more nearly that of the outboard tail configurations, exhibits a rather severe loss of longitudinal stability at a C_L at least 0.2 below the C_L at which the outboard tail configuration has a gradual loss of stability.

Lift, drag, and pitching-moment characteristics.- The lift, drag, and pitching-moment data for one outboard tail configuration are presented in figure 8 for the range of Mach and Reynolds numbers. The tail incidence was constant at -8.0°. The variation of C_L with α (fig. 8(a)) is seen to be very nearly linear up to the maximum angle of attack. The pitching-moment data (fig. 8(b)) show that throughout the range of Mach number and Reynolds numbers, the trend toward instability was gradual and did not approach neutral stability until at least a C_L of 0.8. Lift-drag ratios are presented in figure 8(d) for the wing-body combination, the wing-body-tail-boom configuration with wing fences, and the trimmed values for the tail-on configuration. The maximum values of L/D for the wing-body-tail-boom configuration with wing fences are very nearly equal to those of the tail-off configuration of reference 2 (not presented) which

had a longer fuselage and much larger fences. Also shown in figure 8(d) for M = 0.80 and 0.90 are the maximum trimmed lift-drag ratios for the conventional tail configuration of reference 2 which are slightly lower than those indicated for the outboard tail configuration.

Tail effectiveness and average downwash.- From equation (1) it is seen that the tail contribution to longitudinal stability is a function of both $[1 - (d\epsilon/d\alpha)]$ and $\eta_t q_t/q$. A decrease in $d\epsilon/d\alpha$ would increase the tail contribution to longitudinal stability. To investigate the variation of average downwash and $\eta_t q_t/q$ with lift coefficient, the pitching-moment characteristics of the model with the large outboard tail in the forward position at spanwise station 0.5 b/2 were measured with the tail set at four angles of incidence and with the tail removed. These data are presented in figure 9 for several Mach and Reynolds numbers. The average effective downwash was calculated from the data by means of the expression:[1]

$$\epsilon = \alpha + i_t - \frac{\left(C_{m_{\text{tail on}}} - C_{m_{\text{tail off}}}\right)_{\alpha = \text{const}}}{\partial C_m/\partial i_t} \tag{2}$$

The quantity $[1 - (d\epsilon/d\alpha)]$ was then determined from plots of ϵ versus α. The factor $\eta_t q_t/q$ is given by

$$\frac{\eta_t q_t}{q} = \frac{1}{a_t \bar{V}_t} \frac{\partial C_m}{\partial i_t} \tag{3}$$

In the calculations a_t was taken as 0.50 (ref. 7).

The values of $[1 - (d\epsilon/d\alpha)]$, $\eta_t q_t/q$ and $(dC_m/dC_L)_{\text{trimmed}}$ for the complete model are presented in figure 10 along with the pitching-moment data for the complete model and for the model with the horizontal tail removed. These quantities are also presented at two Mach numbers for the conventional tail configuration of reference 2 which utilized three large wing fences. The data for the outboard tail indicated that the tail contribution to the pitching moment increased with angle of attack for angles greater than that at which the pitching moment of the tail-off configuration had a large unstable trend. A corresponding large increase in $[1 - (d\epsilon/d\alpha)]$ occurred at about the same angle of attack for all test conditions except M = 0.20 where the increase was more

[1]This is the downwash, ϵ, behind the wing with a twist distribution which, due to aeroelastic effects, varies with angle of attack and tail incidence. Since the wing load distribution was not measured, the change in twist due to the wing loads is unknown. The tail booms were statically loaded at the position of the tail surfaces and it was determined that the maximum tail loads at each Mach number produced a change of about 0.35° in the twist at 0.5 b/2.

gradual. As was shown in reference 1, this change in $[1 - (d\epsilon/d\alpha)]$ is a direct result of the loss of lift due to separation on the outer sections of the sweptback wing. For the wing of this investigation, aeroelastic effects may also be a factor. The data of reference 2 show that the opposite effect occurs at the conventional tail position since the lift-curve slopes of the inboard section of the wing tend to increase with increasing angle of attack. The decrease in $[1 - (d\epsilon/d\alpha)]$ for the low-speed condition at an angle of attack of about 17° may be due to the outboard tail surfaces emerging from the wing wake or to the manner in which separation progresses on the wing.

The factor $\eta_t q_t/q$ remained fairly constant over the range of angles of attack investigated. The values of the present investigation are greater than those of reference 2 although both curves have about the same variation with angle of attack. It should be pointed out that the values of a_t assumed in both cases are questionable so that the shape of the curves is more important than absolute magnitudes. With the exception of the data for $M = 0.80$, the curves indicate a favorable increase in $\eta_t q_t/q$ with increasing angle of attack for both the conventional and outboard tail configurations.

The variation of $(dC_m/dC_L)_{trimmed}$ indicates the magnitude of the stability changes which occurred over the range of angles of attack for both the outboard and conventional configurations. Figures 10(a) and 10(d) show that the large changes in stability which occurred between 5° and 10° angle of attack were less severe for the outboard tail configuration than for the conventional tail configuration (see also fig. 7). This could be due to the difference in fence arrangement or to a compensating effect of the outboard tails.

Effects of Flaps and Spoilers

In an attempt to increase the C_L at which the model exhibited at least neutral longitudinal stability at low speeds, trailing-edge flaps which extended from the fuselage to the tail booms and several inboard spoiler configurations were tested in combination with the large tail at spanwise station 0.5 b/2. It was reasoned that the spoilers could increase the longitudinal stability of the configuration either directly as a result of decreasing the lift on the inboard sections of the wing or indirectly through a decrease in the downwash at the tail. The pitching-moment data are presented in figure 11 for the model with the large outboard tails in the forward position at 0.5 b/2 with a fence on the wing leading edge at the tail boom and with several spoiler configurations. For comparative purposes data are also presented for the configuration without spoilers and for the configuration with fences at 0.30 and 0.75 b/2. None of the spoiler configurations was as effective as the fences in improving the pitching-moment characteristics of the model.

[redacted]

The effects of partial-span trailing-edge flaps on the longitudinal characteristics of the model with the large tail in the rear position at 0.5 b/2 are presented in figure 12. The increase in the C_L at which $dC_m/dC_L = 0$ was about 0.2. The lift-drag ratio at $C_L = 1.0$ of the configuration with flaps was about 4.5 as compared to about 3.4 for the configuration without flaps. Flaps thus could be used at low speeds to increase the stability and the lift-drag ratios at high lift coefficients.

Lateral Effectiveness of Outboard Horizontal Tails

The effects of varying the tail incidence of the left horizontal tail with the right tail removed are shown in figure 13 for one Mach number. The effectiveness of differential deflection of the horizontal tails as indicated by $\Delta C_l/\Delta i_t$ decreased by about 25 percent as the angle of attack was increased from 0° to 20°. The damping in roll of the wing-body outboard-tail configuration at zero angle of attack was calculated by the method of reference 8 and an estimate was made of the wing-tip helix angle, pb/2V, resulting from differential deflection of the horizontal tails. The results of these calculations indicated that a differential deflection of 20° would result in a value of pb/2V of about 0.09 at zero angle of attack, which indicates that the outboard tail is an effective roll control. Yawing moments resulting from differential deflection of the horizontal tails were not considered in this calculation.

Comparison of Sideslip Characteristics of Outboard and Conventional Tail Configurations

Effects of variable β at constant α.- The effects of varying the angle of sideslip at several angles of attack on the lateral and longitudinal characteristics were determined for an outboard tail configuration, a conventional-tail configuration, and the wing-body combination. The three configurations had the same wing fences at 0.30 b/2 and 0.75 b/2. The data indicate (fig. 14) that the pitching-moment generally increased positively with increasing angle of sideslip at the higher angles of attack for all configurations tested. The outboard tail configuration and the wing-body configuration showed the same general change of pitching moment with angle of sideslip at the low Mach numbers while the conventional tail had a more nearly constant pitching moment. At the higher Mach numbers the pitching moment of the conventional-tail configuration decreased with increasing angle of attack while the pitching moment of the other configurations remained almost constant. The change in pitching moment of the outboard tail configuration from $\beta = 0°$ to $\beta = 15°$ at $\alpha \approx 12.2°$ represents an increase in $(C_L)_{trim}$ of about 0.15.

Data are presented in figures 15, 16, and 17 for several Mach numbers and angles of attack, which show that the variations of C_l, C_n, and C_Y with β were approximately linear for the three configurations tested. The effective dihedral was positive (except at $\alpha = 0$) for the three configurations and either the conventional or outboard tails provided directional stability to at least 9° of sideslip at Mach numbers up to 0.90 and angles of attack up to 12°. When the data obtained with the conventional and outboard tail configuration are compared, it should be noted that the combined area of the two outboard vertical tails was only 47 percent of the area of the conventional tail and the tail volume coefficient, $\overline{V}_v$, was 0.060 as compared to 0.112.

Effects of variable α at constant β.- The variation of pitching-moment coefficient with angles of attack at several Mach numbers and sideslip angles is presented in figure 18. The improved pitching-moment characteristics of the outboard tail configuration, as compared to the conventional tail configuration, are apparent at all Mach numbers and angles of sideslip. As expected from the data of figure 15, changing sideslip angle from -6° to -12° had little or no effect on the pitching-moment characteristics of the three configurations tested.

The variation of the quantity C_n/β, used here as a measure of the directional stability, is presented as a function of angle of attack for several Mach numbers and sideslip angles in figure 19. The directional stability increment due to the outboard vertical tails increased at the higher angles of attack at all Mach numbers and angles of sideslip. In contrast, the directional stability increment due to the conventional vertical tail was more nearly constant over the angle-of-attack range at all test conditions.

For the three configurations tested, the quantity C_l/β, used here as a measure of the effective dihedral, decreased with increasing angle of attack in a fairly uniform manner up to about 5° (fig. 20). Above this angle, there was, in general, a reduction in the rate of change of C_l/β with α. In general, C_l/β for the outboard tail configuration had the same variation with angle of attack as the wing-body combination. Both configurations had a small positive value of C_l/β at zero angle of attack (see figs. 15 and 20). The conventional tail configuration had a negative C_l/β at zero angle of attack and about the same value as the other configurations at 15° angle of attack. The small rolling moment at zero angle of attack for the outboard tail configuration is probably a result of the small vertical lever arm and the small vertical-tail forces as compared to those of the conventional vertical tail.

The quantity C_Y/β is presented in figure 21 for the three configurations tested. As would be expected, the tail contribution to C_Y/β at the higher angles of attack showed the same general characteristics as were exhibited in the tail contribution to C_n/β.

CONCLUDING REMARKS

An investigation has been made of the effects of an unconventional tail arrangement on the subsonic static longitudinal and lateral stability characteristics of an airplane configuration with a 63° sweptback wing of aspect ratio 3.5. Tail booms, extending rearward from approximately the midsemispan of each wing panel, supported independent tail assemblies well outboard of the usual position at the rear of the fuselage. The aerodynamic characteristics of the configuration were not entirely satisfactory, although in many respects the characteristics were considerably better than those of a tailless configuration or one with a fuselage-mounted tail.

The longitudinal stability characteristics of the wing without fences is characterized by a sudden and large decrease in stability at a lift coefficient of about 0.5. The outboard tails reduced but did not eliminate this loss of stability. The addition of wing fences improved the flow on the wing and reduced the severity of the stability decrease of the wing so that the outboard tail configuration was stable to at least a lift coefficient of 0.8 over the range of Mach number and Reynolds numbers of the investigation.

Sideslip angles up to 15° had only small effects upon the pitching-moment characteristics of the outboard tail configuration. There was a favorable increase in the directional stability for the outboard tail configuration at the higher angles of attack as opposed to a decrease in the directional stability of the conventional tail configuration at most Mach numbers and Reynolds numbers of the investigation. The variation of C_l/β with angle of attack was undesirable for both configurations. The data indicate that the outboard tail is an effective roll control.

Ames Research Center
National Aeronautics and Space Administration
Moffett Field, Calif., Dec. 4, 1958

REFERENCES

1. Edwards, George G., and Savage, Howard F.: A Horizontal-Tail Arrangement For Counteracting Static Longitudinal Instability of Sweptback Wings. NACA RM A56D06, 1956.

2. Buell, Donald A., and Kolbe, Carl D.: The Effects at Subsonic Speeds of Wing Fences and a Tail on the Longitudinal Characteristics of a 63° Swept-Wing and Fuselage Combination. NACA RM A57E02, 1957.

3. Fournier, Paul G.: Low-Speed Investigation of Static Longitudinal and Lateral Stability Characteristics of an Airplane Configuration With a Highly Tapered Wing and With Several Body and Tail Arrangements. NACA RM L57A08, 1957.

4. Jones, J. Lloyd, and Demele, Fred A.: Aerodynamic Study of a Wing-Fuselage Combination Employing a Wing Swept Back 63° - Characteristics Throughout the Subsonic Speed Range With a Wing Cambered and Twisted for a Uniform Load at a Lift Coefficient of 0.25. NACA RM A9D25, 1949.

5. Sivells, James C., and Salmi, Rachel M.: Jet-Boundary Corrections for Complete and Semispan Swept Wings in Closed Circular Wind Tunnels. NACA TN 2454, 1951.

6. Herriot, John G.: Blockage Corrections for Three-Dimensional-Flow Closed-Throat Wind Tunnels, With Consideration of the Effects of Compressibility. NACA Rep. 995, 1950. (Supersedes NACA RM A7B28)

7. Ross, J. G., Hills, R., and Lock, R. C.: Wind Tunnel Tests on a 90° Apex Delta Wing of Variable Aspect Ratio (Sweepback 36.8°). British A.R.C. CP 83 (Rep. 12,666 and 12,000), 1952. (Also R.A.E. Aero 2333, Aug. 1949)

8. Campbell, John P., and McKinney, Marion O.: Summary of Methods for Calculating Dynamic Lateral Stability and Response and for Estimating Lateral Stability Derivatives. NACA Rep. 1098, 1952. (Supersedes NACA TN 2409)

TABLE I.- MOMENT CENTERS AND TAIL VOLUME COEFFICIENTS

Horizontal tail	Tail spanwise position, percent b/2	Moment center, percent $\bar{c}$	Horizontal-tail length, $l_t/\bar{c}_w$	Horizontal-tail volume coefficient, $S_t l_t/S_w \bar{c}_w$	Vertical-tail volume coefficient, $S_v l_v/S_w b_w$
Off		25			
Small	50	37	1.962	0.169	
Medium	40	35	1.289	.149	
Medium	40	35	1.635	.188	
Medium	50	34	1.646	.190	
Medium	50	37	1.962	.226	
Large	50	40	1.586	.289	0.060
Large	50	43	1.903	.347	
Conventional	0	42	1.412	.308	.112

[redacted]

TABLE II.- GEOMETRIC PROPERTIES OF THE MODEL

Wing	
Aspect ratio	3.50
Taper ratio	0.25
Sweepback (leading edge), deg	63.0
Airfoil (in streamwise direction)	NACA 64A005
Span, ft	3.750
Area, sq ft	4.018
Mean aerodynamic chord, ft	1.200
Outboard horizontal and vertical tails	
Airfoil (in streamwise direction)	NACA 0004-64
Sweepback (leading edge), deg	45.0
Taper ratio	0.25
Span (one tail), ft	
Large	0.938
Medium	0.745
Small	0.645
Vertical (to plane of wing leading edge), ft	0.548
Area (total), sq ft	
Large	0.733
Medium	0.463
Small	0.347
Vertical	0.500
Aspect ratio	
Horizontal tails	2.40
Vertical tails	0.60
Conventional horizontal tail	
Airfoil	NACA 0004-64
Taper ratio	0.33
Aspect ratio	4.00
Area, sq ft	0.876
Span, ft	1.868
Sweepback (0.50 chord line)	0
Conventional vertical tail	
Airfoil	NACA 0003.5-64
Taper ratio	0.16
Aspect ratio	1.51
Area, sq ft	1.067
Span (to fuselage center line), ft	1.269
Sweepback (leading edge), deg	54.0

[redacted]

[redacted]

TABLE II.- GEOMETRIC PROPERTIES OF THE MODEL - Concluded

Fuselage

Fineness ratio	
Long fuselage	12.0
Short fuselage	10.9
Base area, sq ft	0.130

Coordinates[1] (long fuselage)

Distance from nose, in.	Radius, in.
0	0
5	.80
10	1.44
15	1.94
20	2.32
25	2.60
30	2.79
35	2.90
40	2.97
45	2.99
51.25	3.00
57.75	3.00
61.75	2.99
65.75	2.90
69.75	2.67
72.00	2.44

[1]Removable section from 51.25 to 57.75 inches from nose.

[redacted]

A-22395

(a) Outboard tails and fences.

Figure 1.- Photograph of the model in the wind tunnel.

A-22396

(b) Outboard tails, fences, and flaps.

Figure 1.- Concluded.

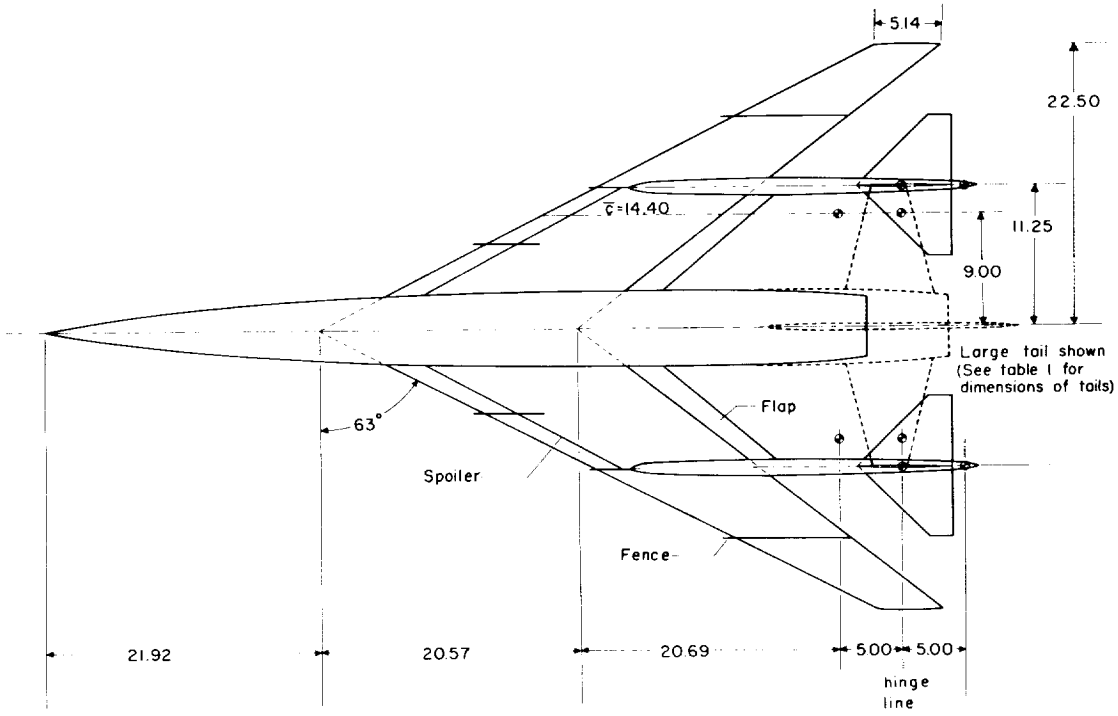

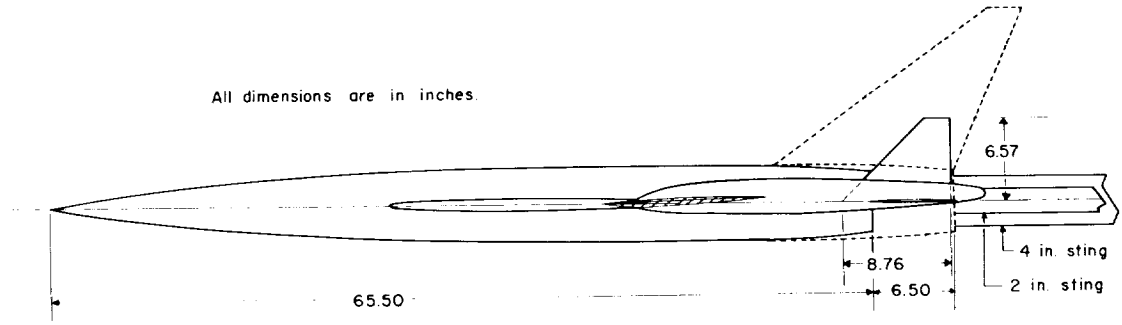

(a) Plan and side views.

Figure 2.- Geometry of the model.

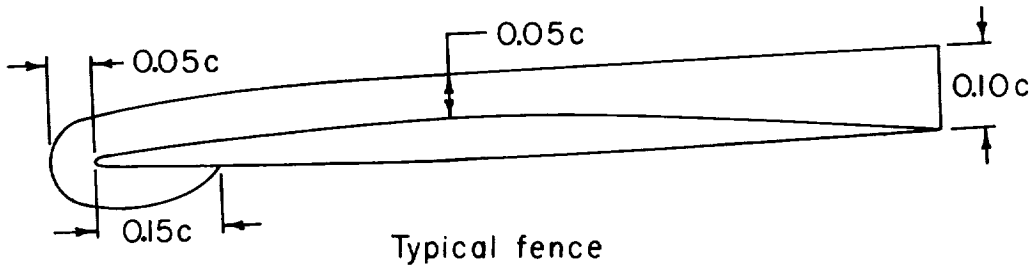

Typical fence

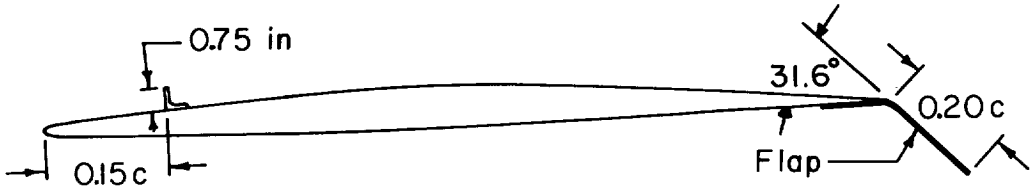

Spoiler and flap

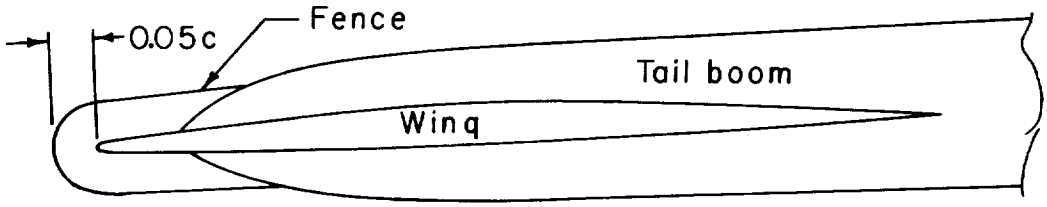

Juncture of wing and tail boom

(b) Model details.

Figure 2.- Concluded.

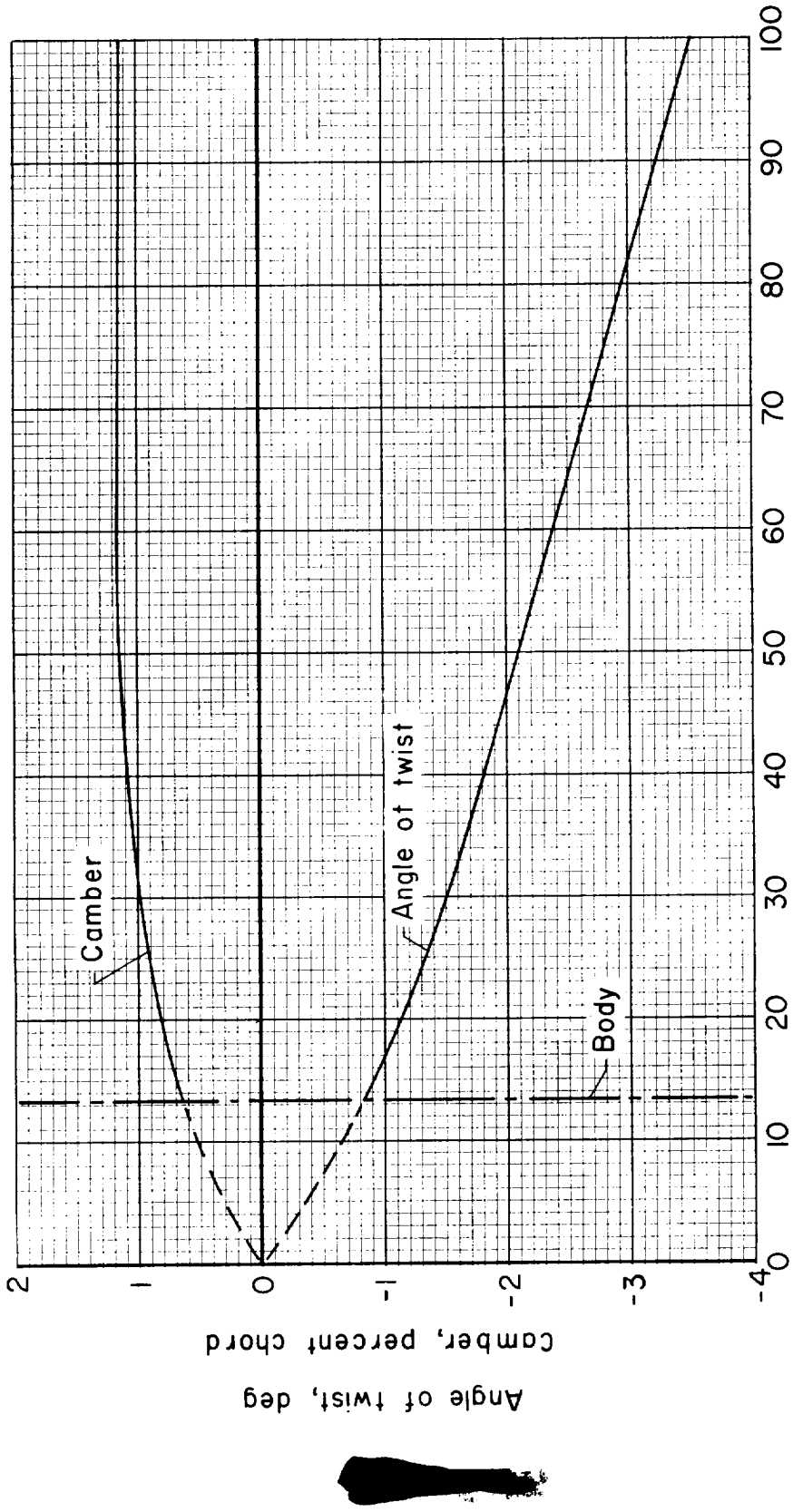

Figure 3.- Camber and twist of the wing.

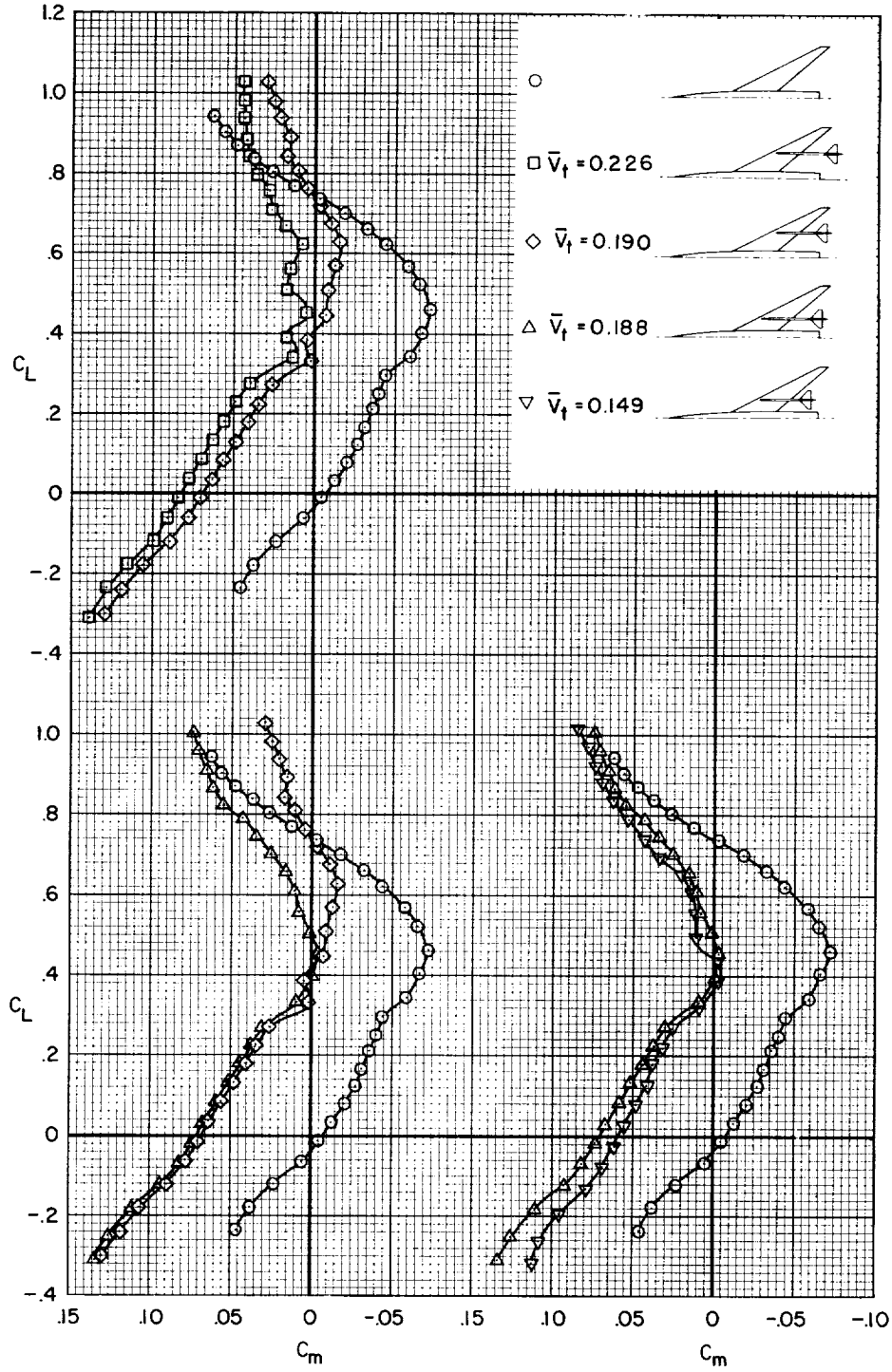

Figure 4.- The effects of changing the longitudinal and lateral position of the medium outboard tails on the pitching-moment characteristics of the model; $i_t = -10^\circ$, M = 0.46, R = 3,500,000.

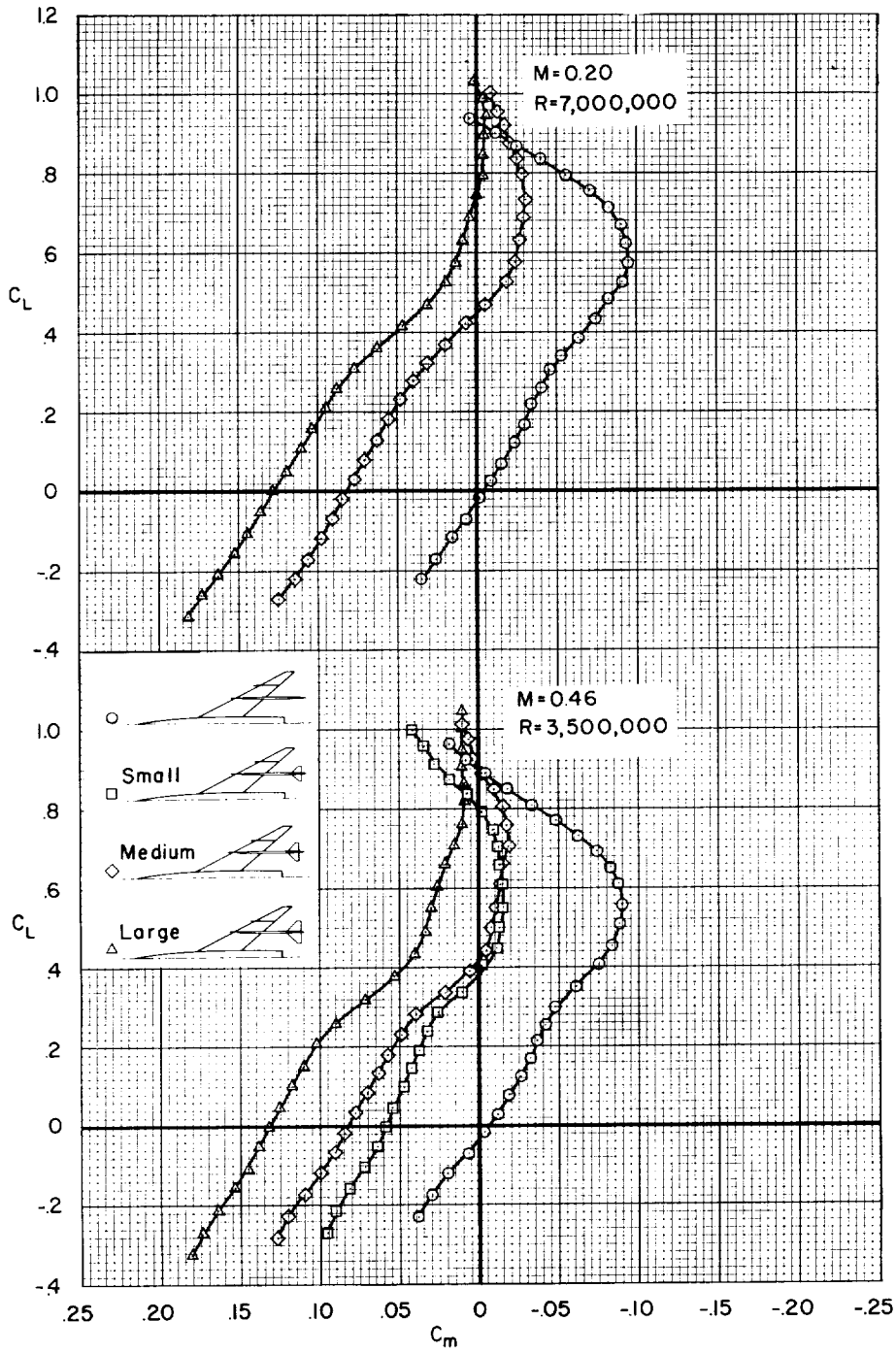

(a) M = 0.20 and 0.46

Figure 5.- The effects of tail size on the pitching-moment characteristics of the model; tails in the rear position at 0.5 b/2; $i_t = -10^\circ$.

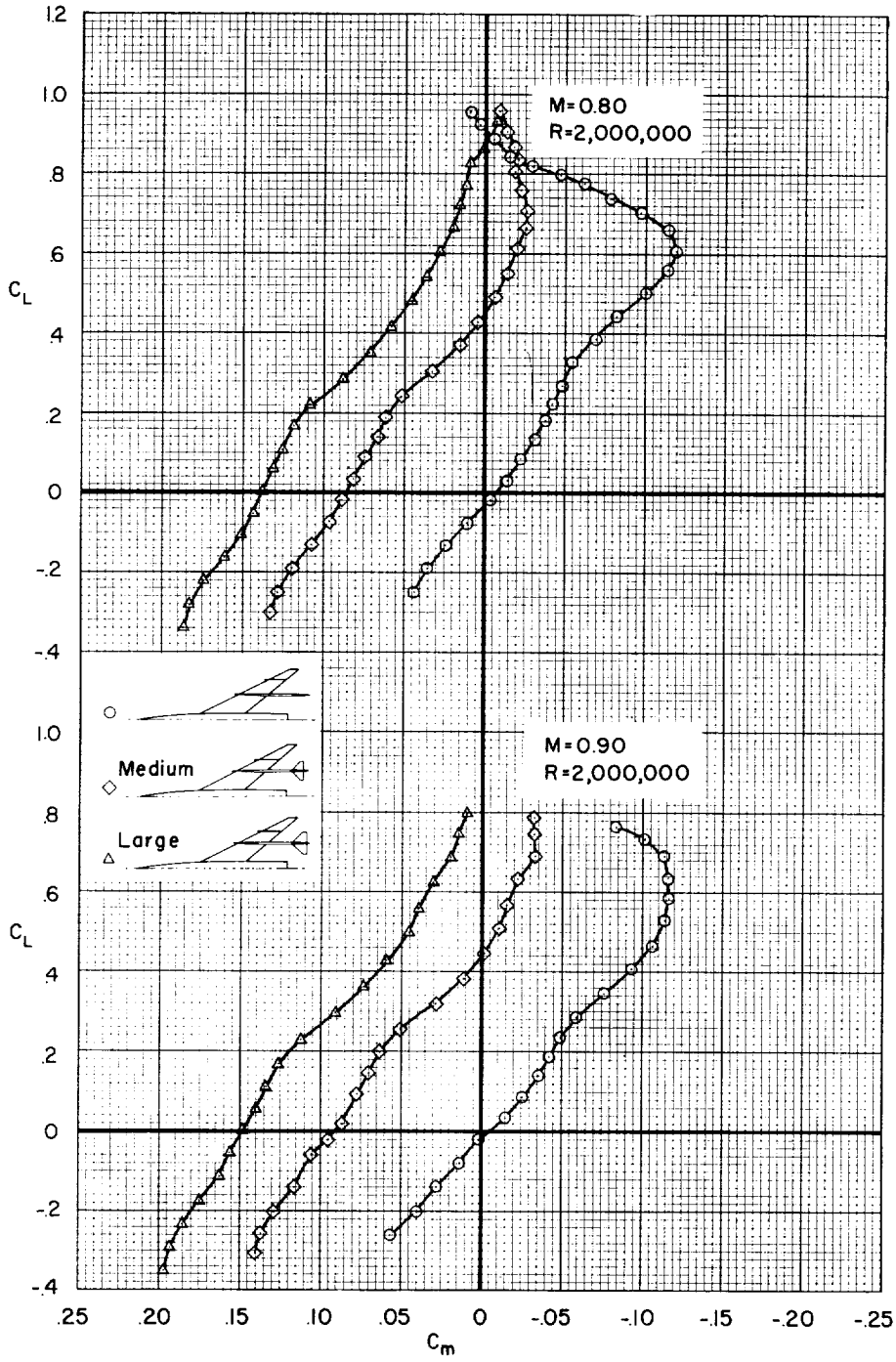

(b) M = 0.80 and 0.90

Figure 5.- Concluded.

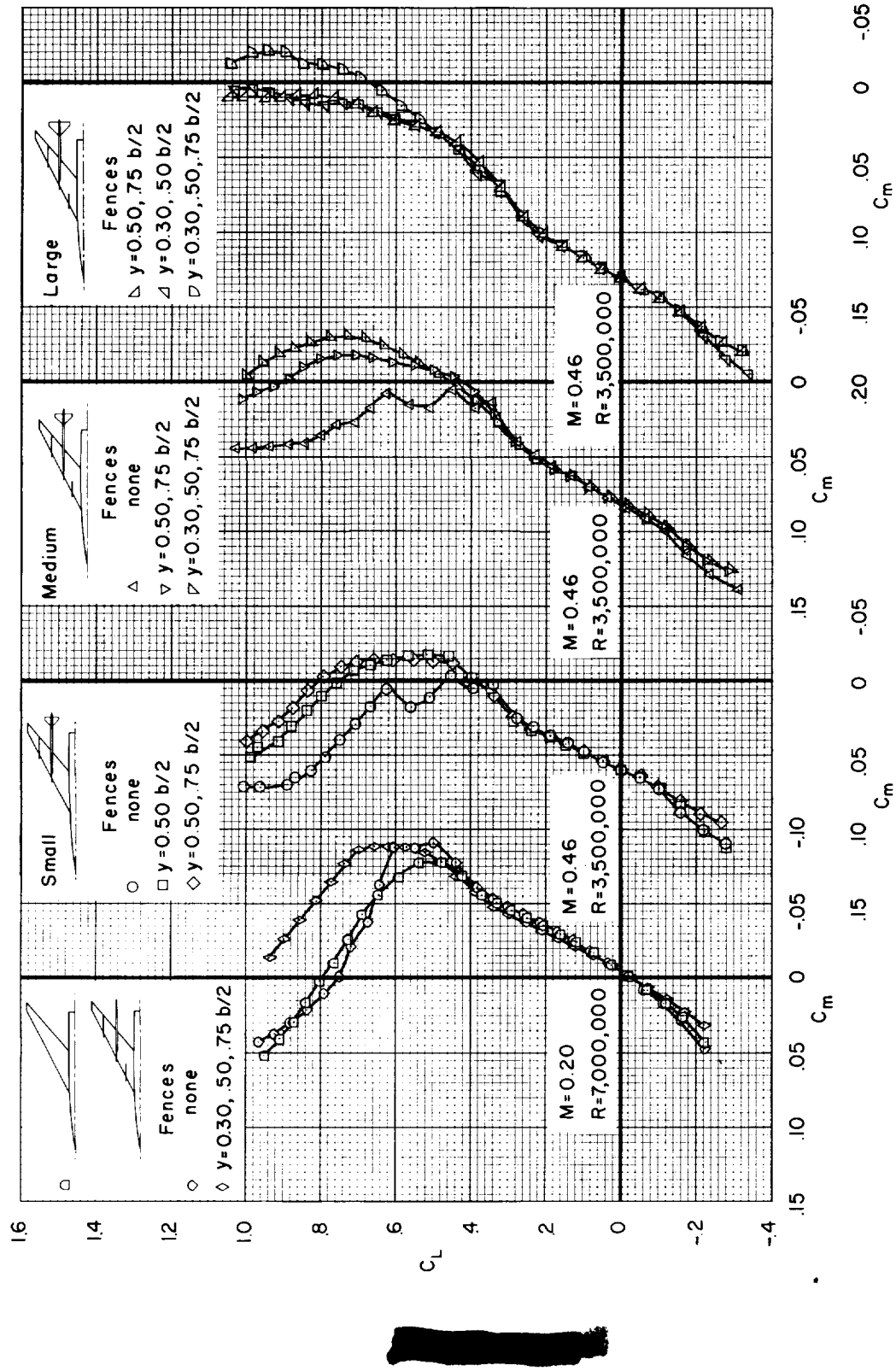

Figure 6.- The effects of wing fences on the pitching-moment characteristics of the model with the outboard tails in the rear position at 0.5 b/2; $i_t = -10^\circ$.

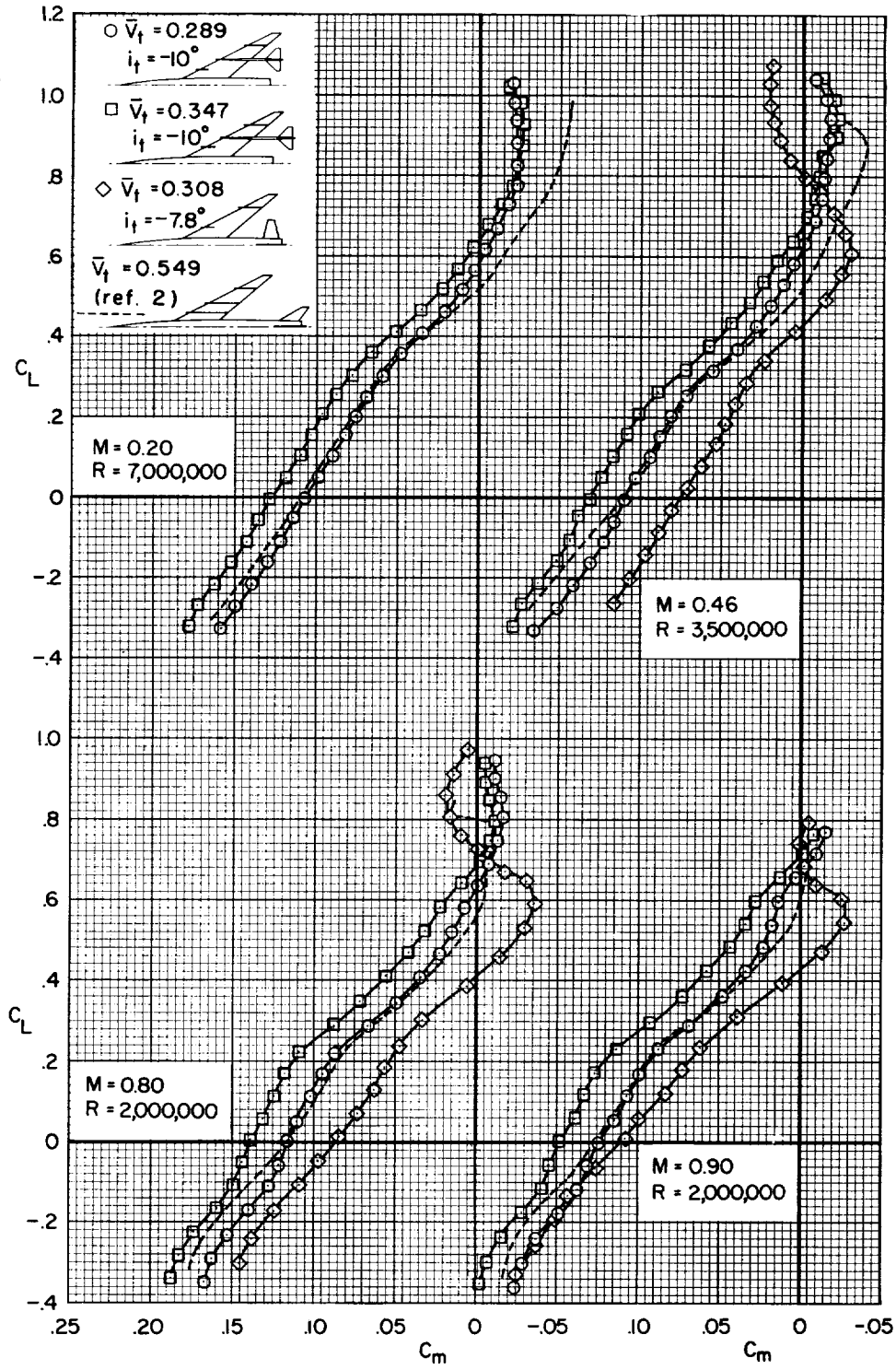

Figure 7.- Comparison of the pitching-moment characteristics of two outboard tail configurations and two conventional tail configurations.

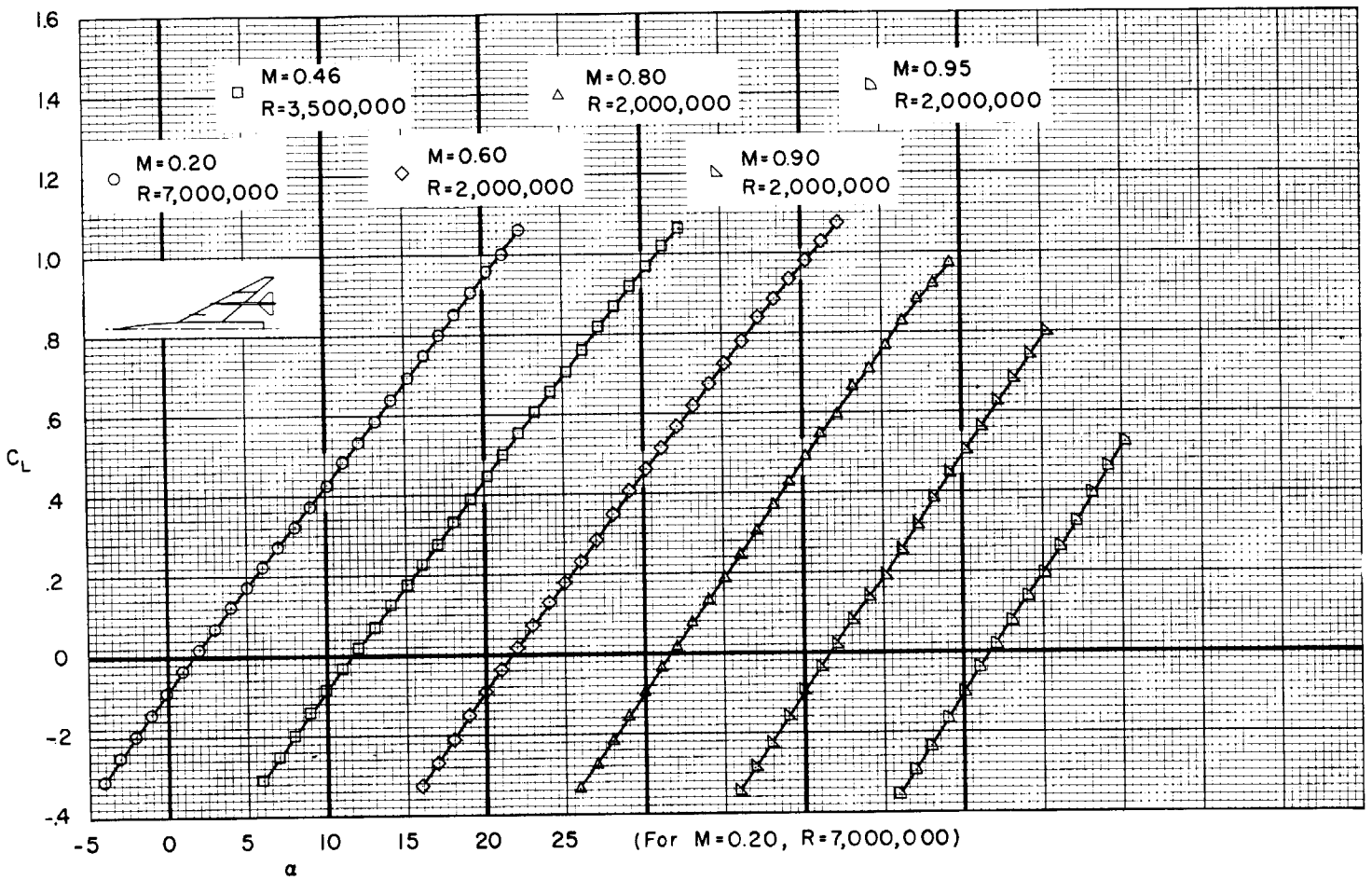

(a) α vs. C_L

Figure 8.- The effects of Mach and Reynolds numbers on the lift, pitching-moment, drag, and lift-drag characteristics of the model with the large tail in the forward position at 0.5 b/2; $i_t = -8^\circ$.

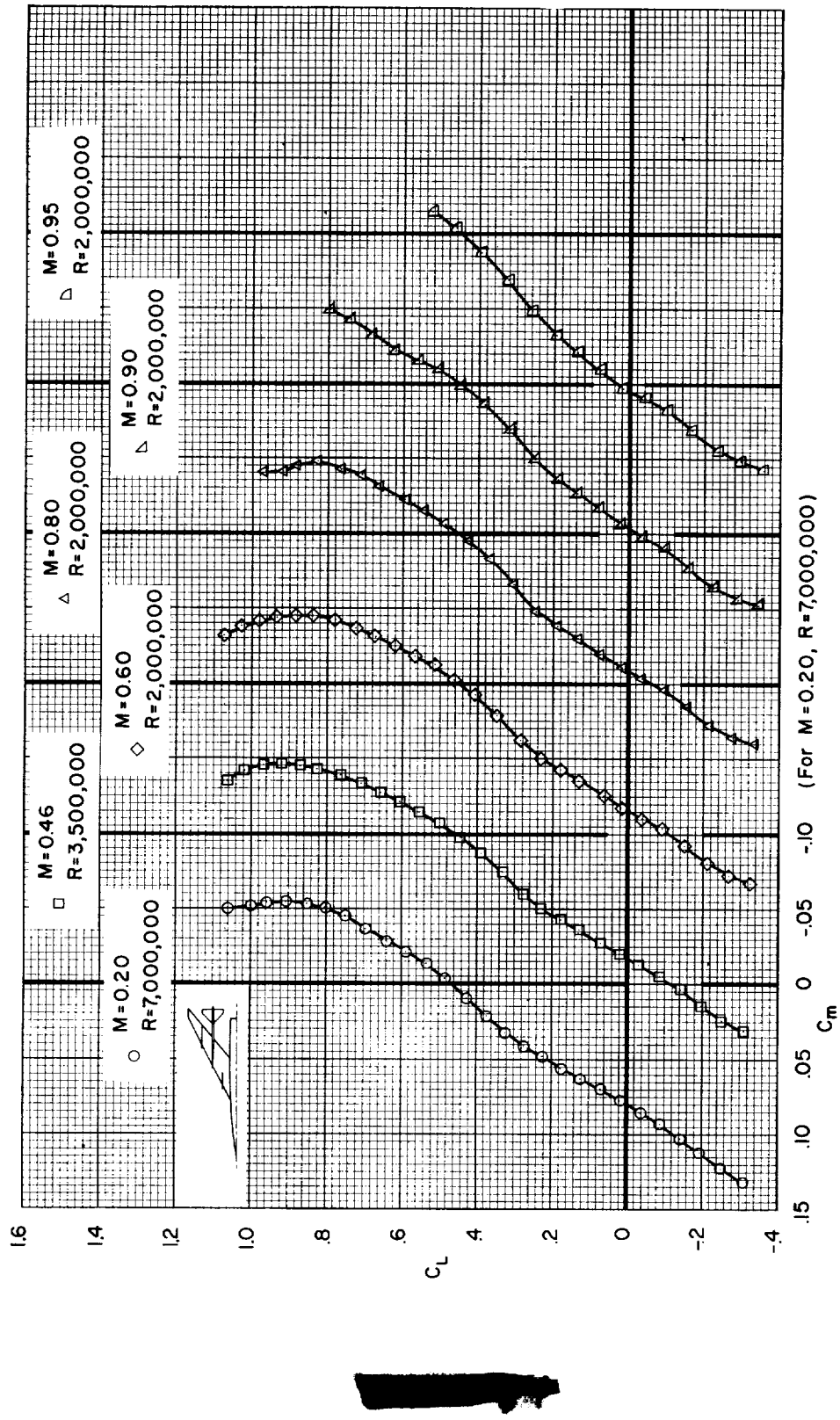

(b) C_m vs. C_L

Figure 8.- Continued.

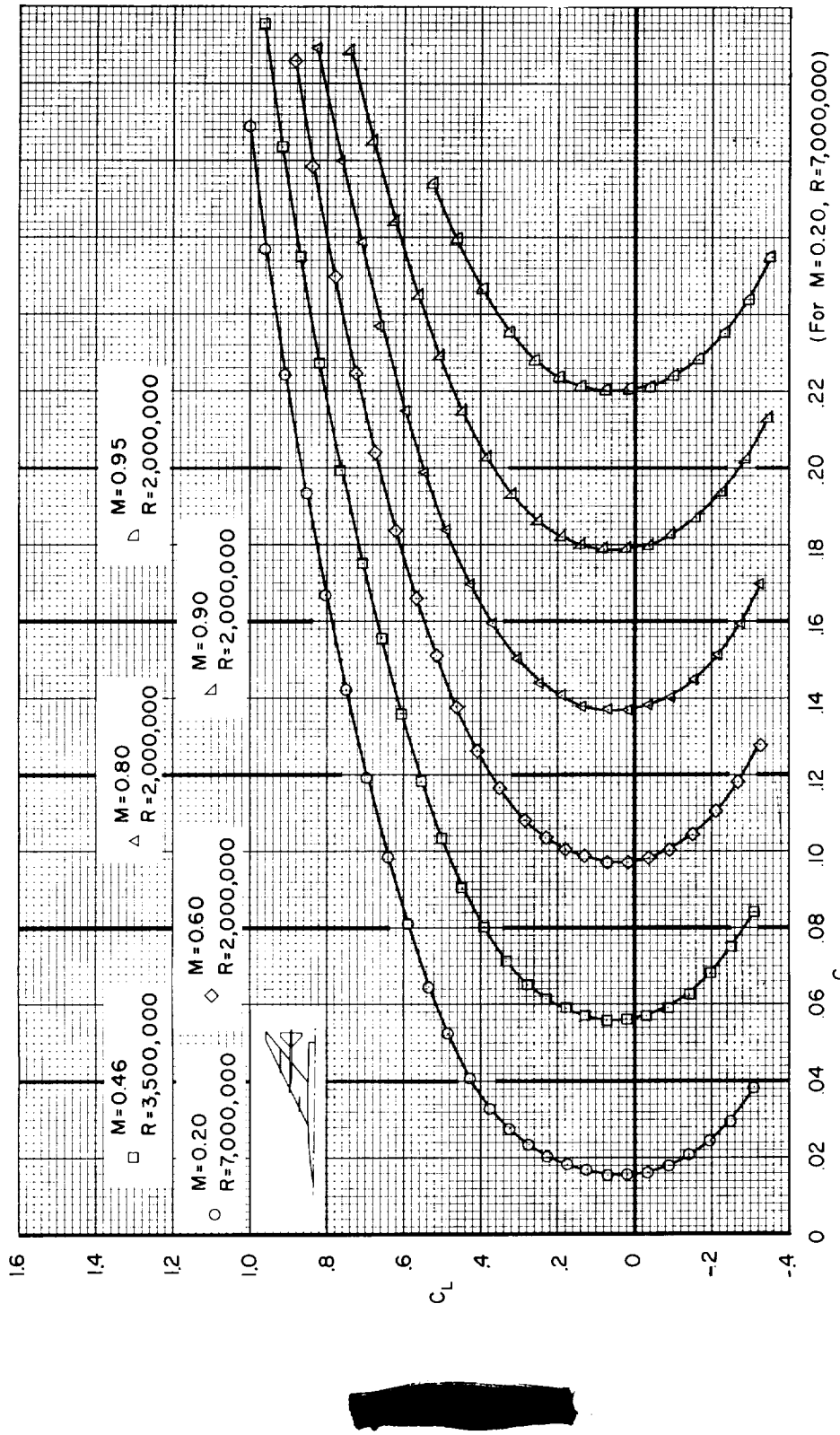

(c) C_D vs. C_L

Figure 8.- Continued.

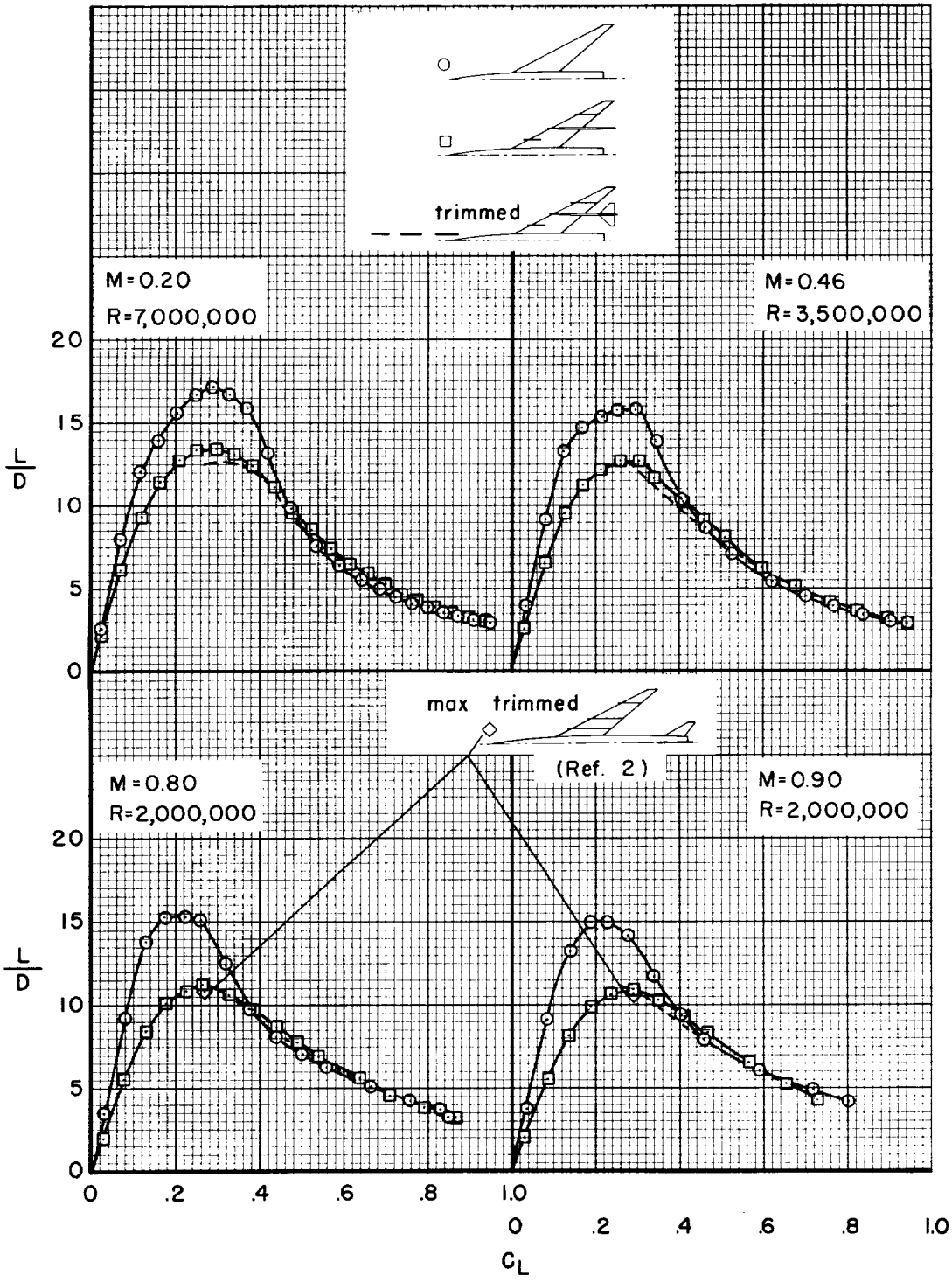

(d) L/D vs. C_L

Figure 8.- Concluded.

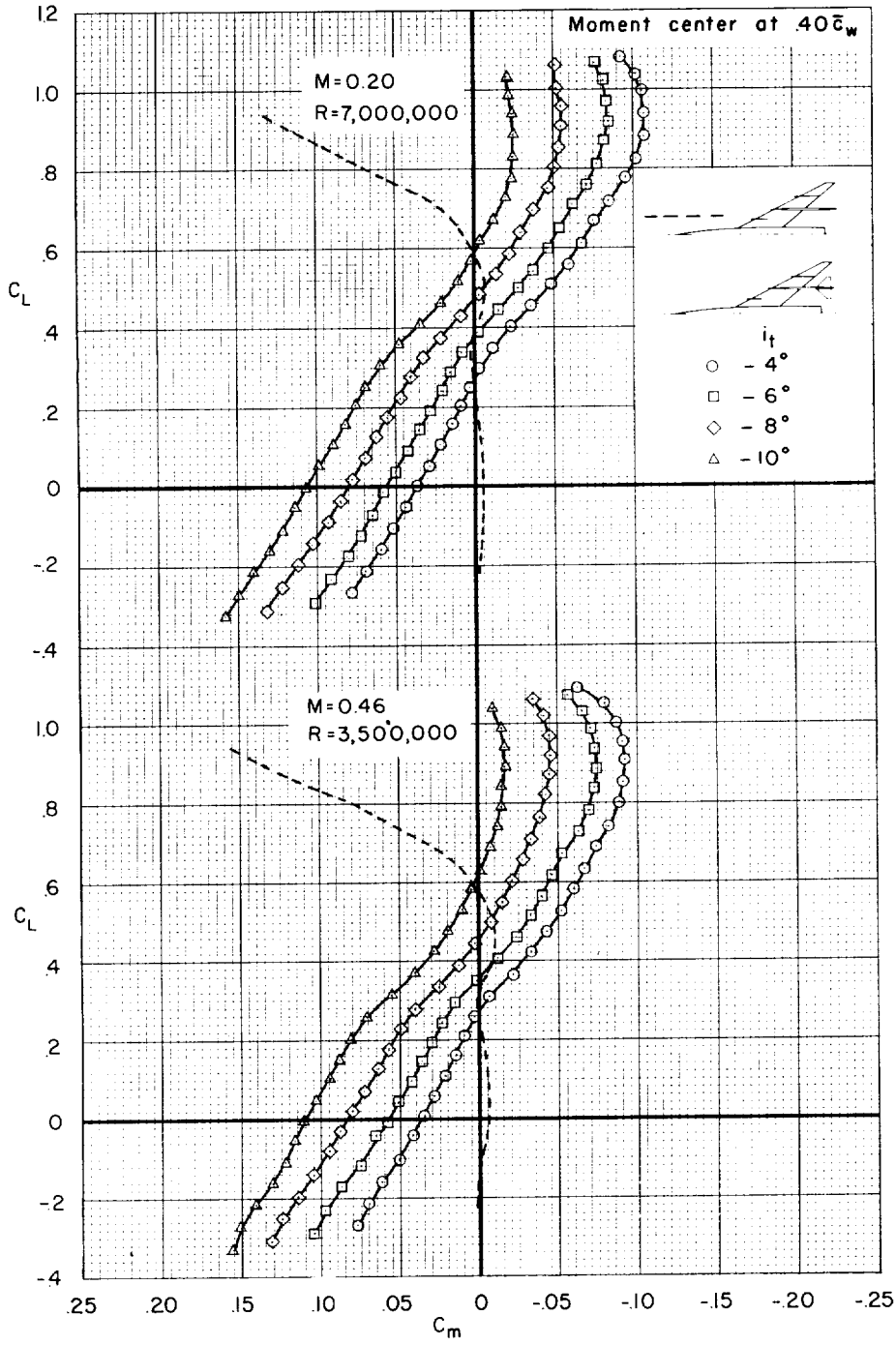

(a) M = 0.20 and 0.46

Figure 9.- The pitching-moment characteristics of the model with the large tail at several incidences; tails in forward position at 0.5 b/2.

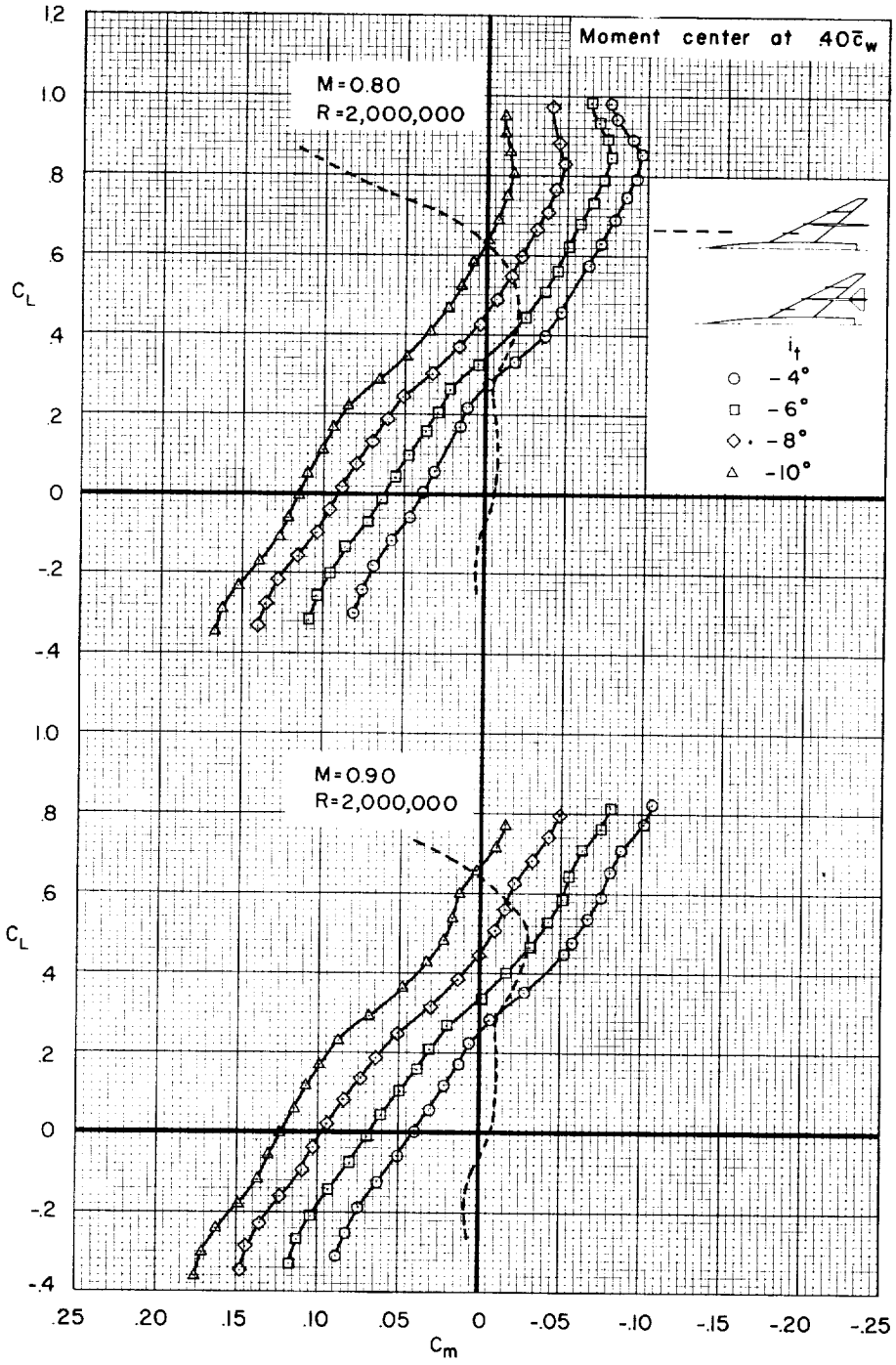

(b) M = 0.80 and 0.90

Figure 9.- Concluded.

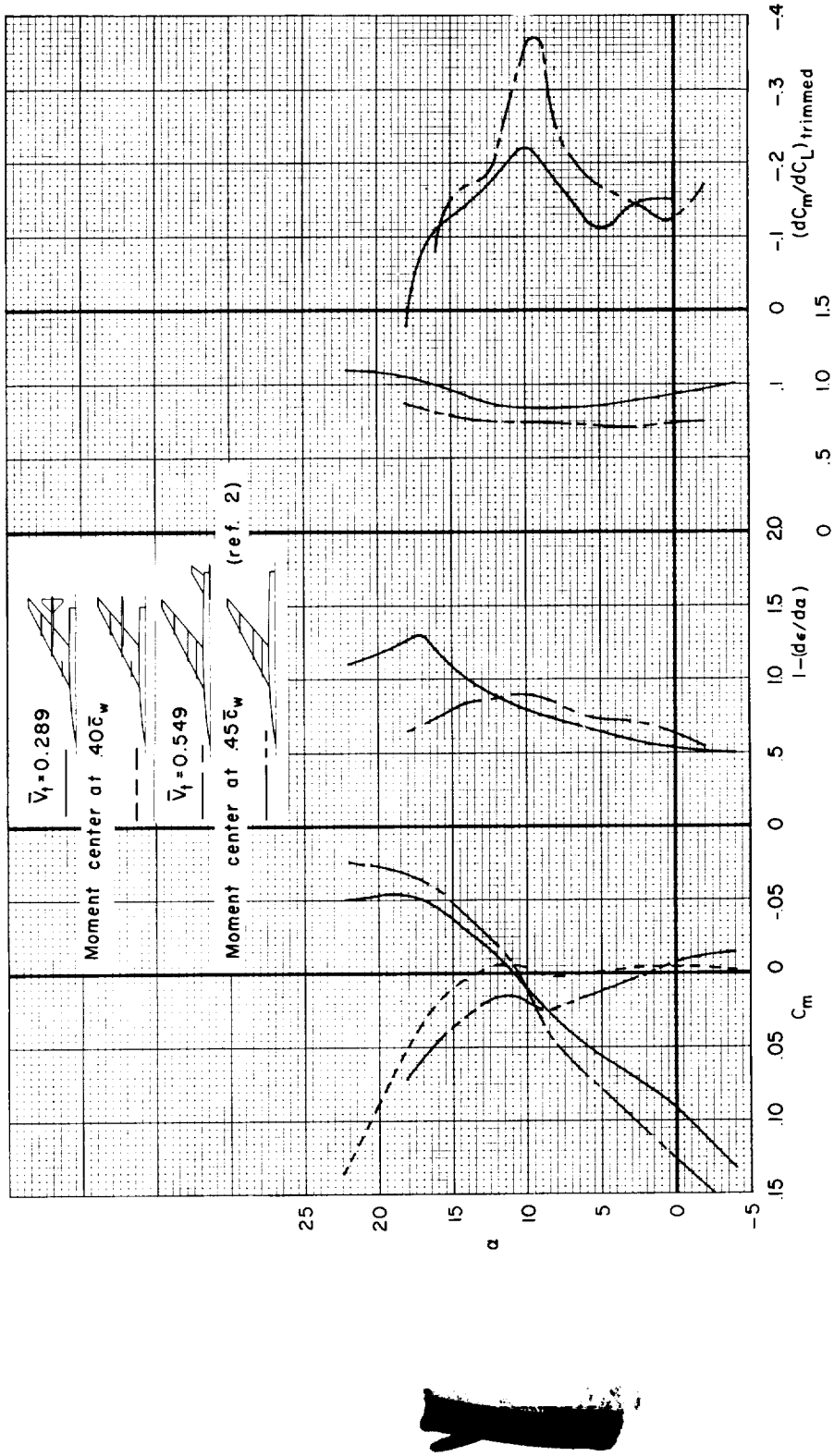

(a) M = 0.20, R = 7,000,000

Figure 10.- The variation with angle of attack of C_m, 1 - $(d\epsilon/d\alpha)$, $\eta_t q_t/q$, and $(dC_m/dC_L)_{trimmed}$ for the model with the large outboard tail in the forward position at 0.5 b/2 and with a conventional tail; $i_t = -8°$.

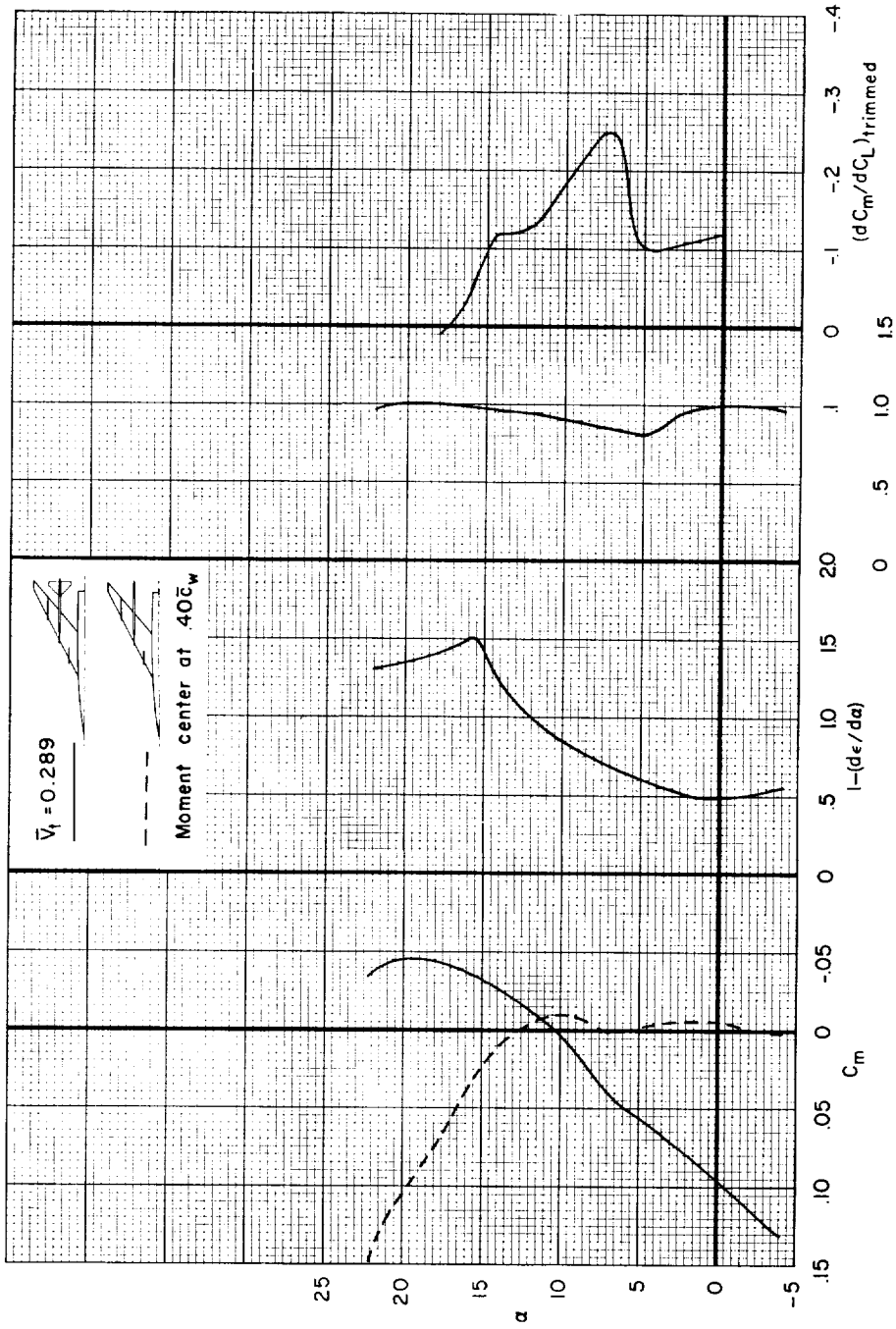

(b) M = 0.46, R = 3,500,000

Figure 10.- Continued.

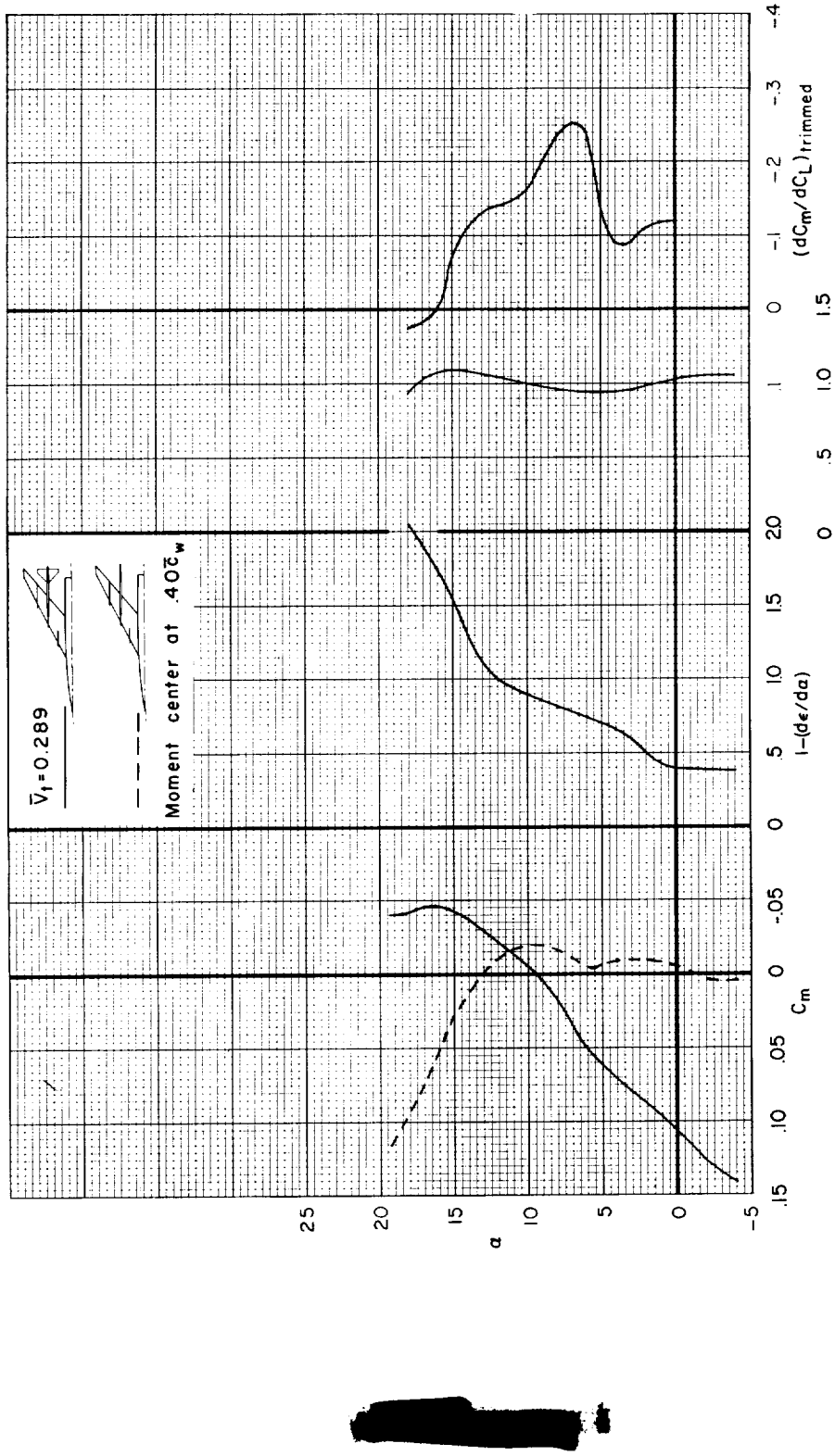

(c) M = 0.80, R = 2,000,000

Figure 10.- Continued.

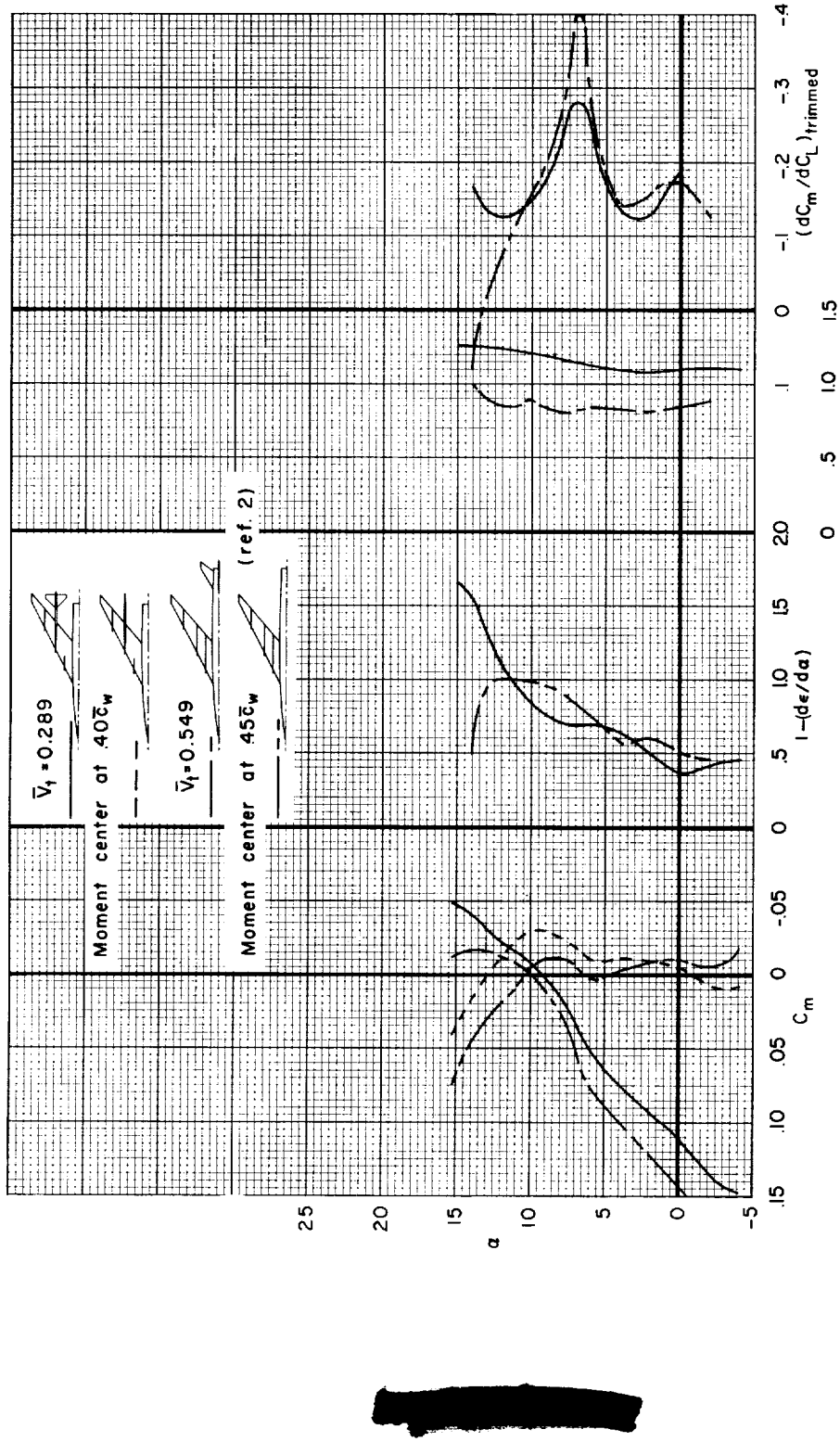

(d) M = 0.90, R = 2,000,000

Figure 10.- Concluded.

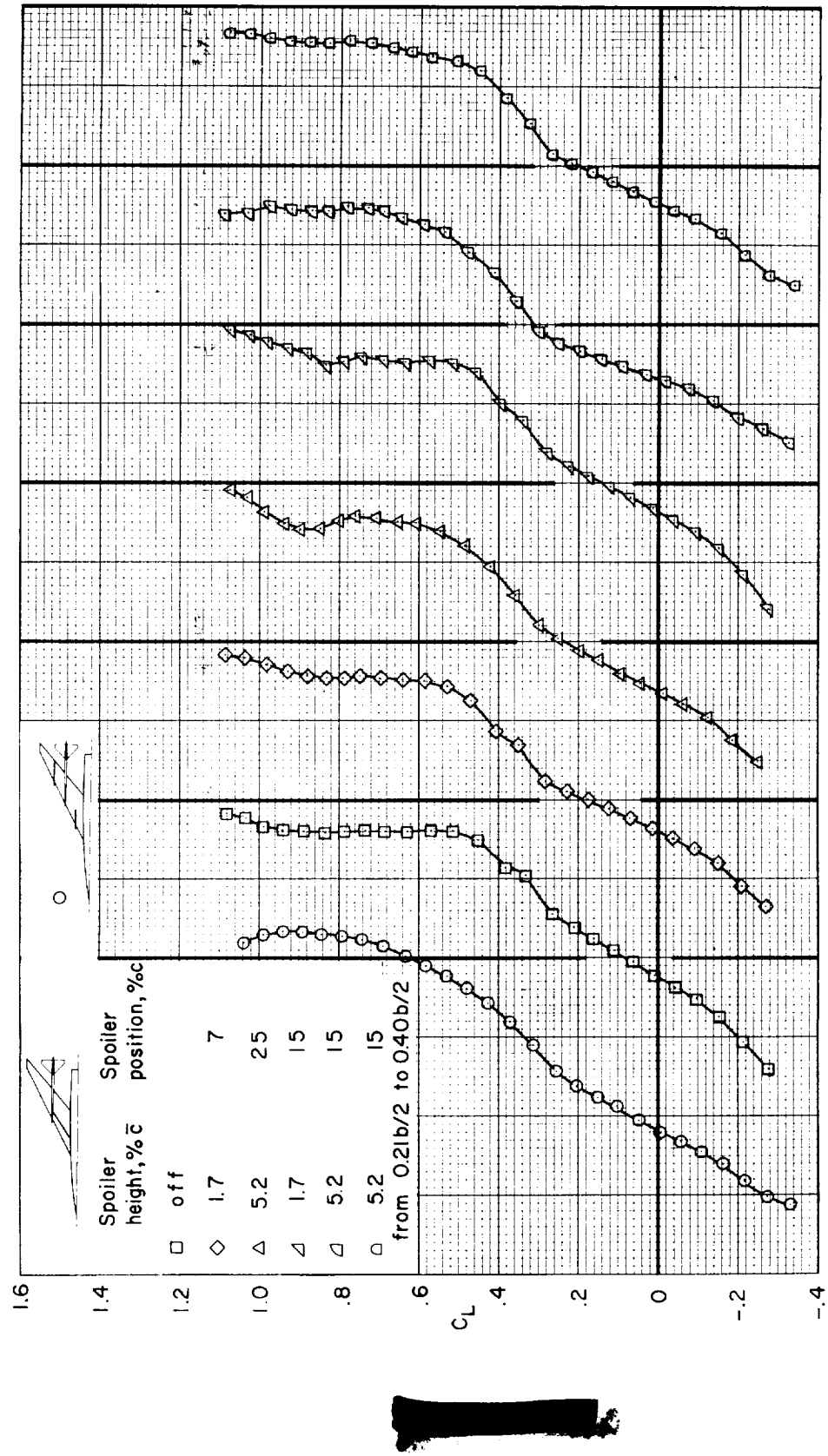

Figure 11.- The effects of several spoiler configurations on the pitching-moment characteristics of the model with the large tail in the forward position at 0.5 b/2; $i_t = -10^\circ$, M = 0.46, R = 3,500,000.

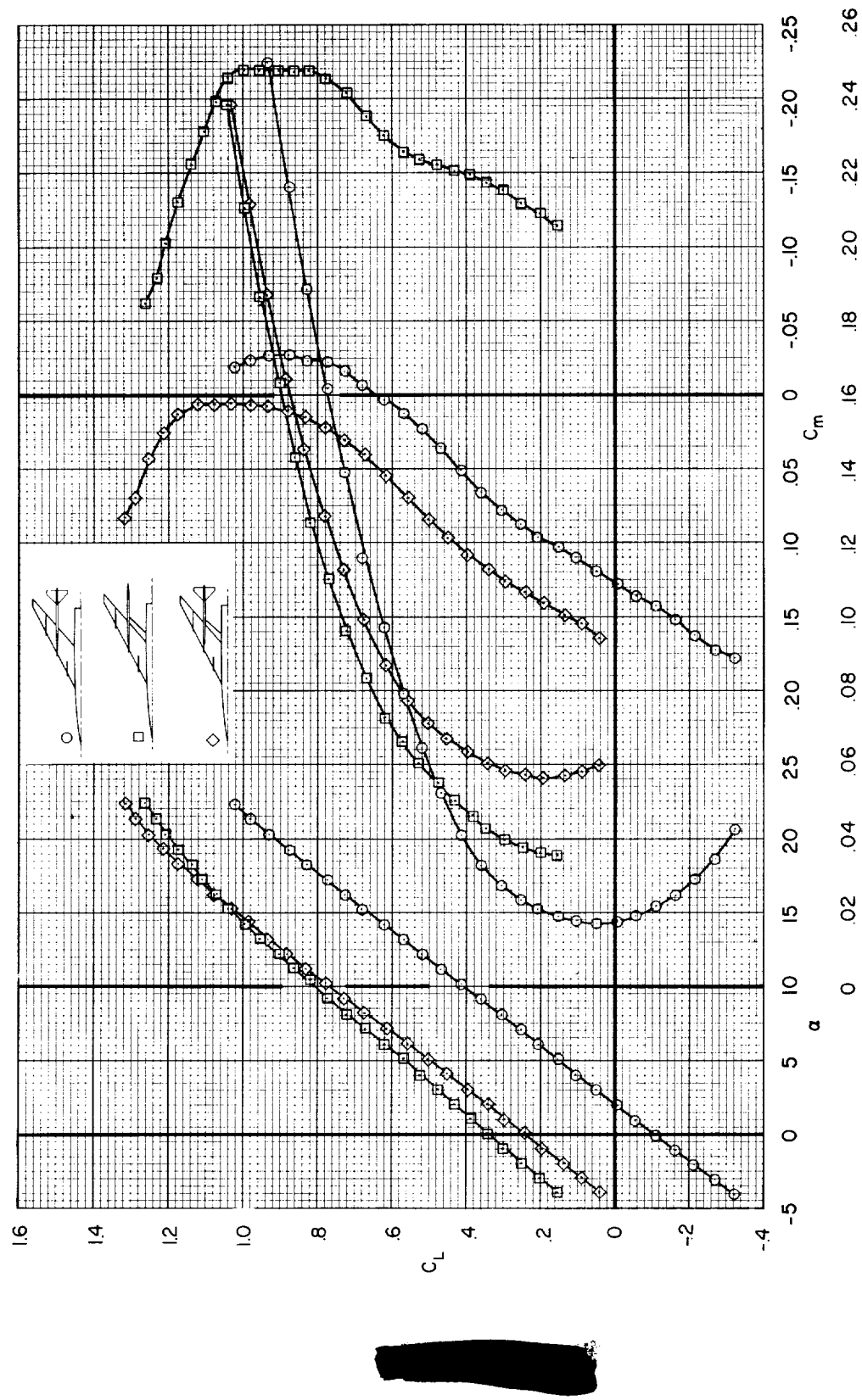

Figure 12.- The effects of flaps on the longitudinal stability characteristics of the model with the large tail in the rear position at 0.5 b/2; $i_t = -10^o$, M = 0.20, R = 7,000,000.

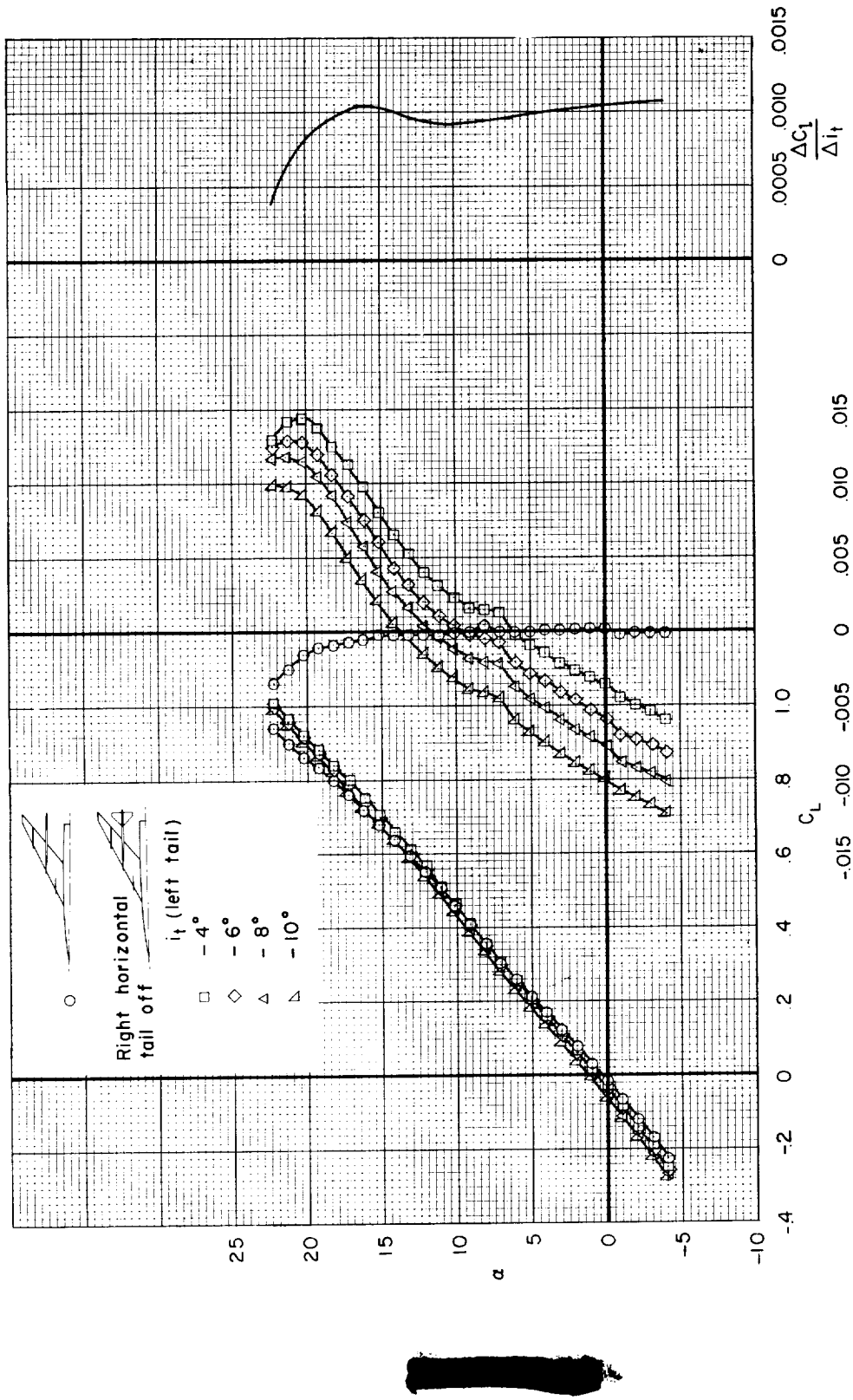

Figure 13.- The effects of varying the incidence of the left horizontal tail in the forward position at 0.5 b/2 with the right horizontal tail removed; large tail, M = 0.46, R = 3,500,000.

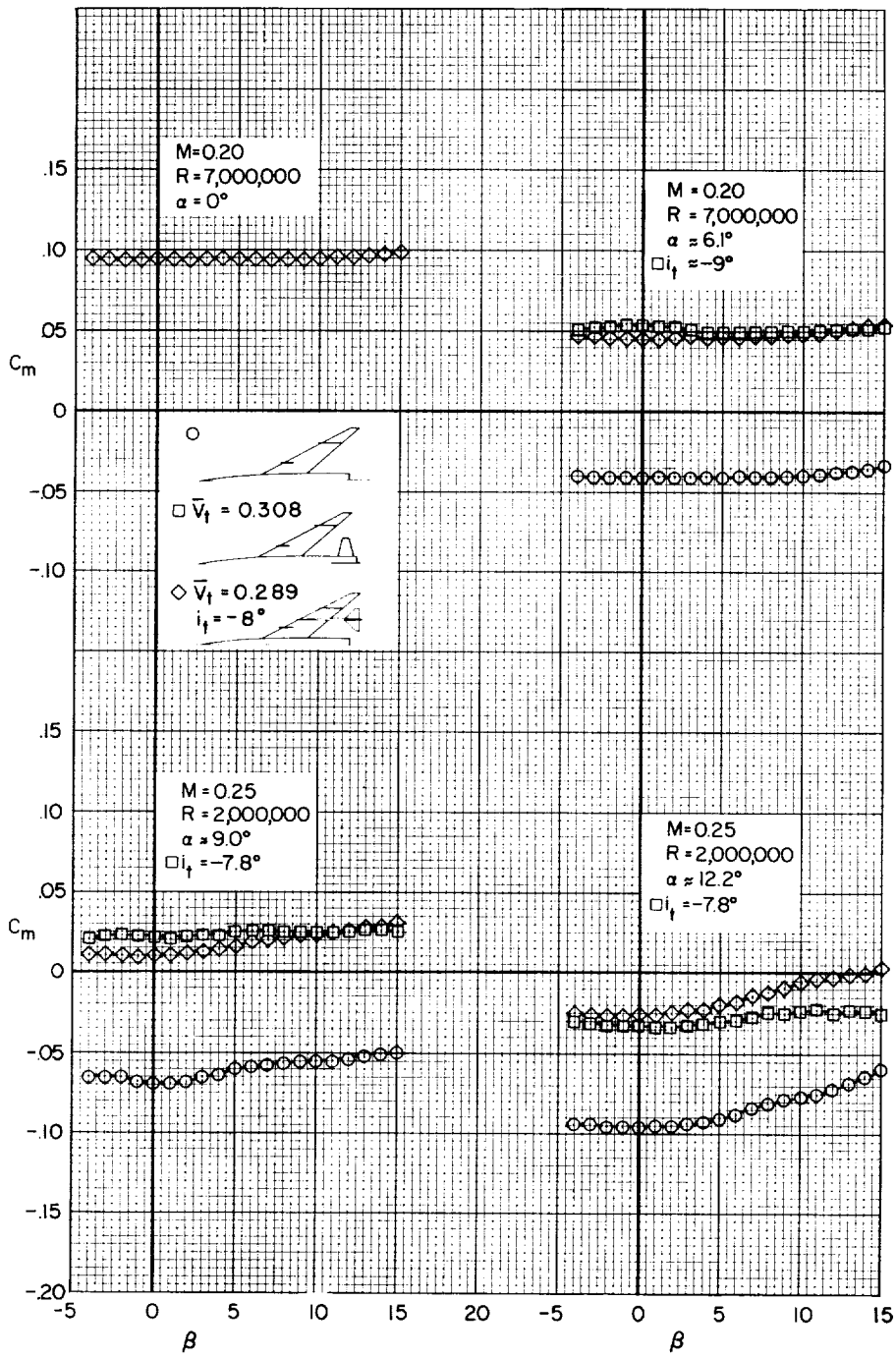

(a) M = 0.20 and 0.25

Figure 14.- The variation with angle of sideslip of the pitching-moment coefficient for the tail off, outboard, and conventional tail configurations.

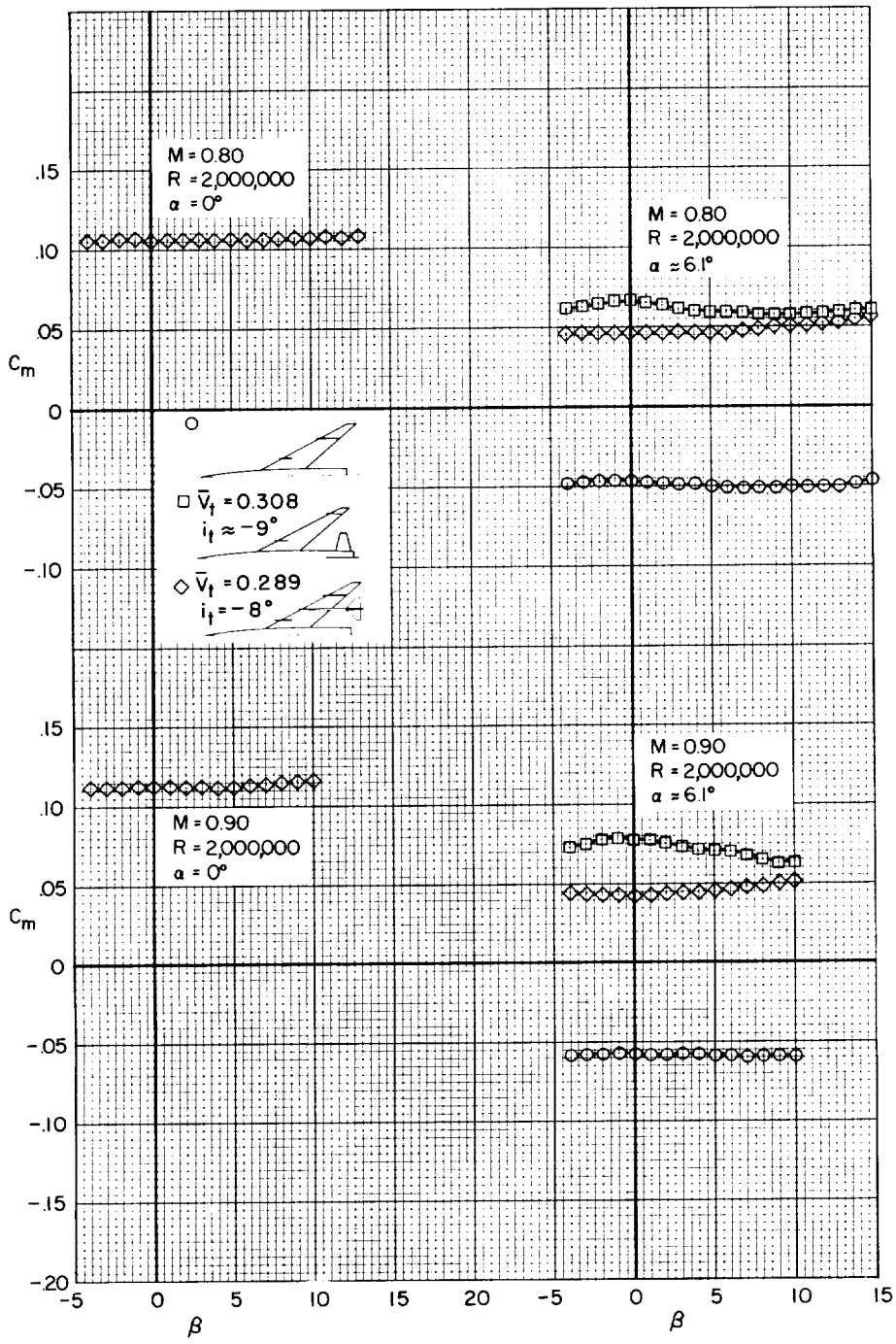

(b) M = 0.80 and 0.90

Figure 14.- Concluded.

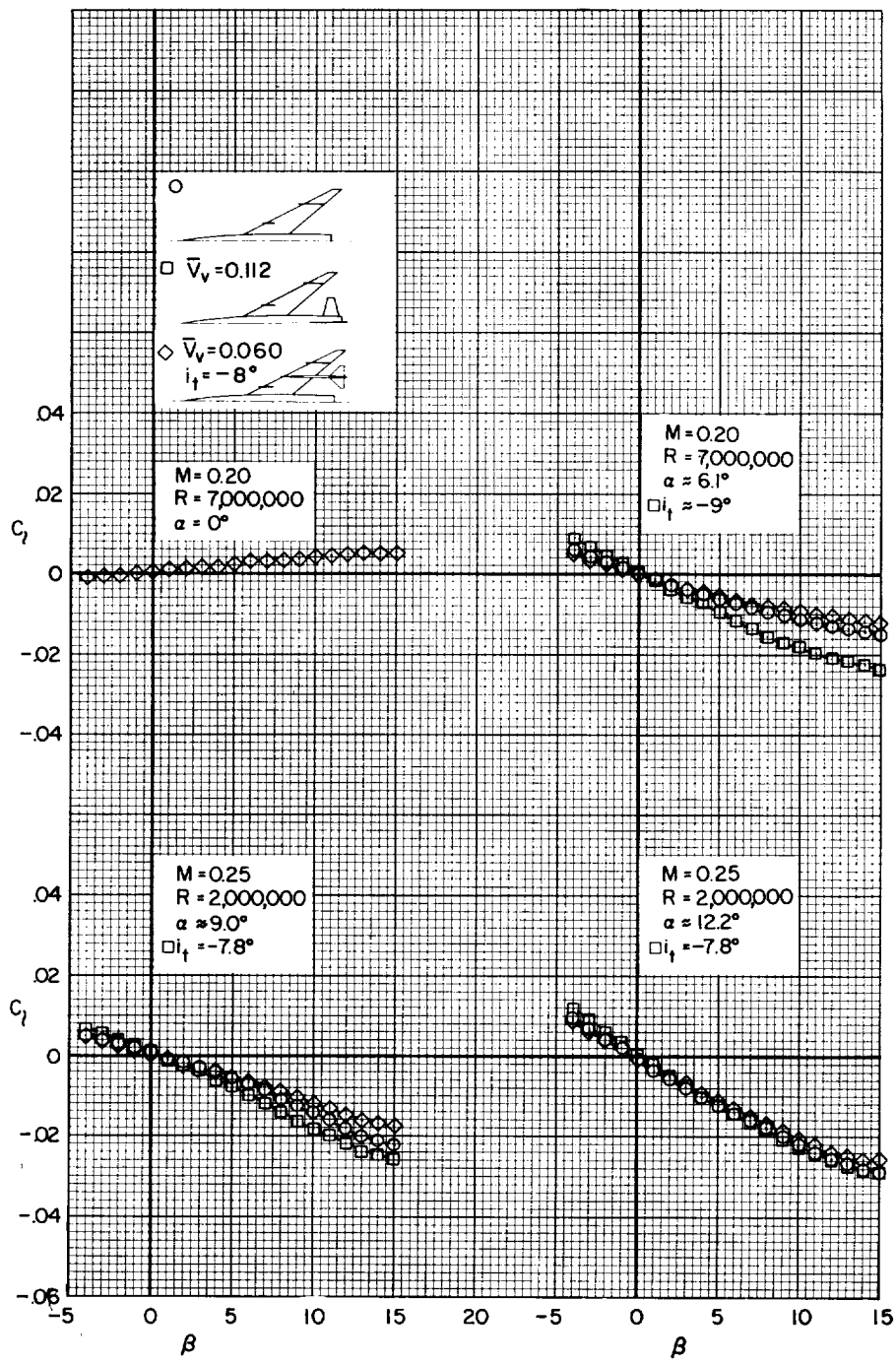

(a) M = 0.20 and 0.25

Figure 15.- The variation with angle of sideslip of the rolling-moment coefficient of the tail off, outboard, and conventional tail configurations.

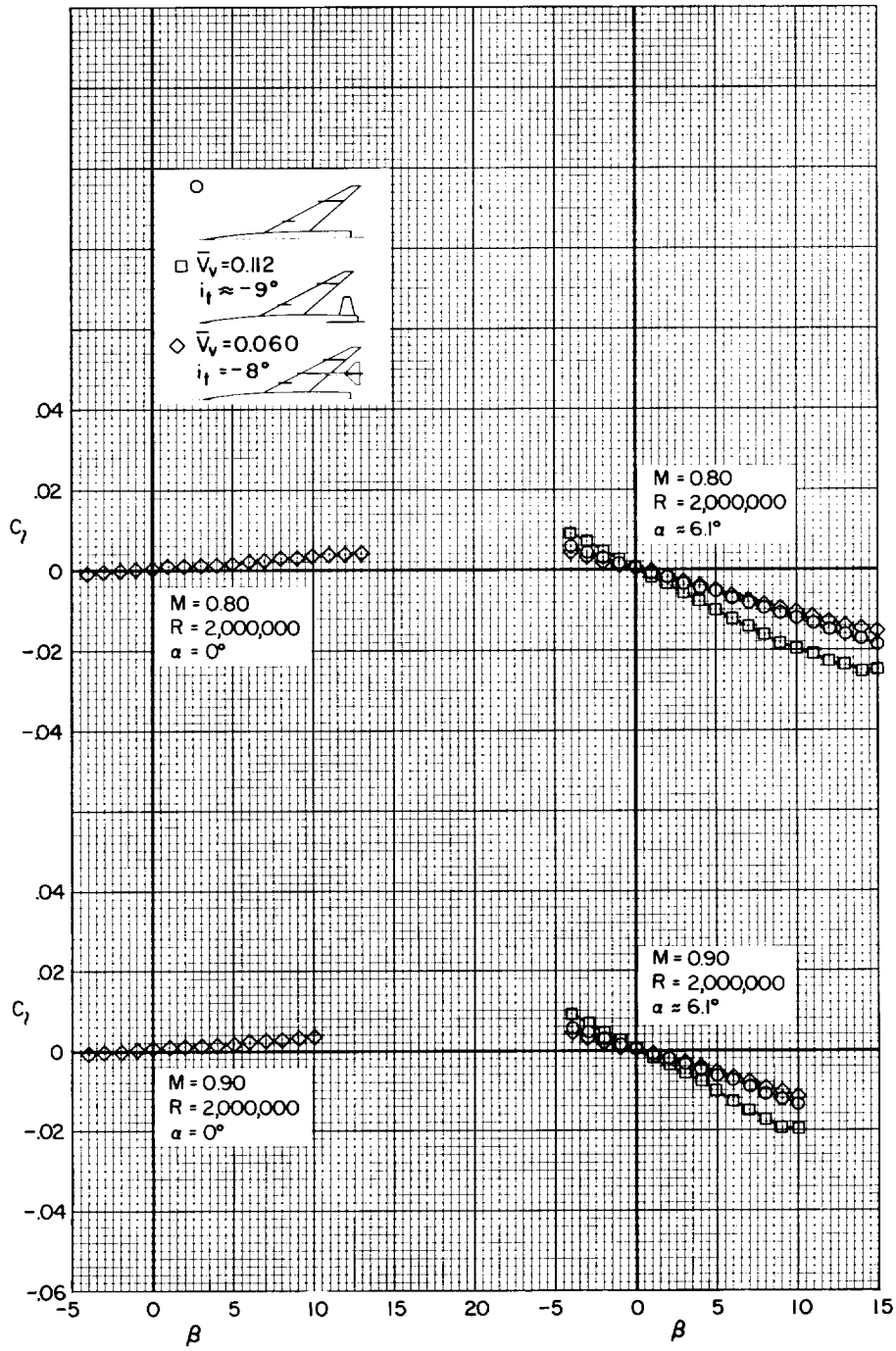

(b) M = 0.80 and 0.90

Figure 15.- Concluded.

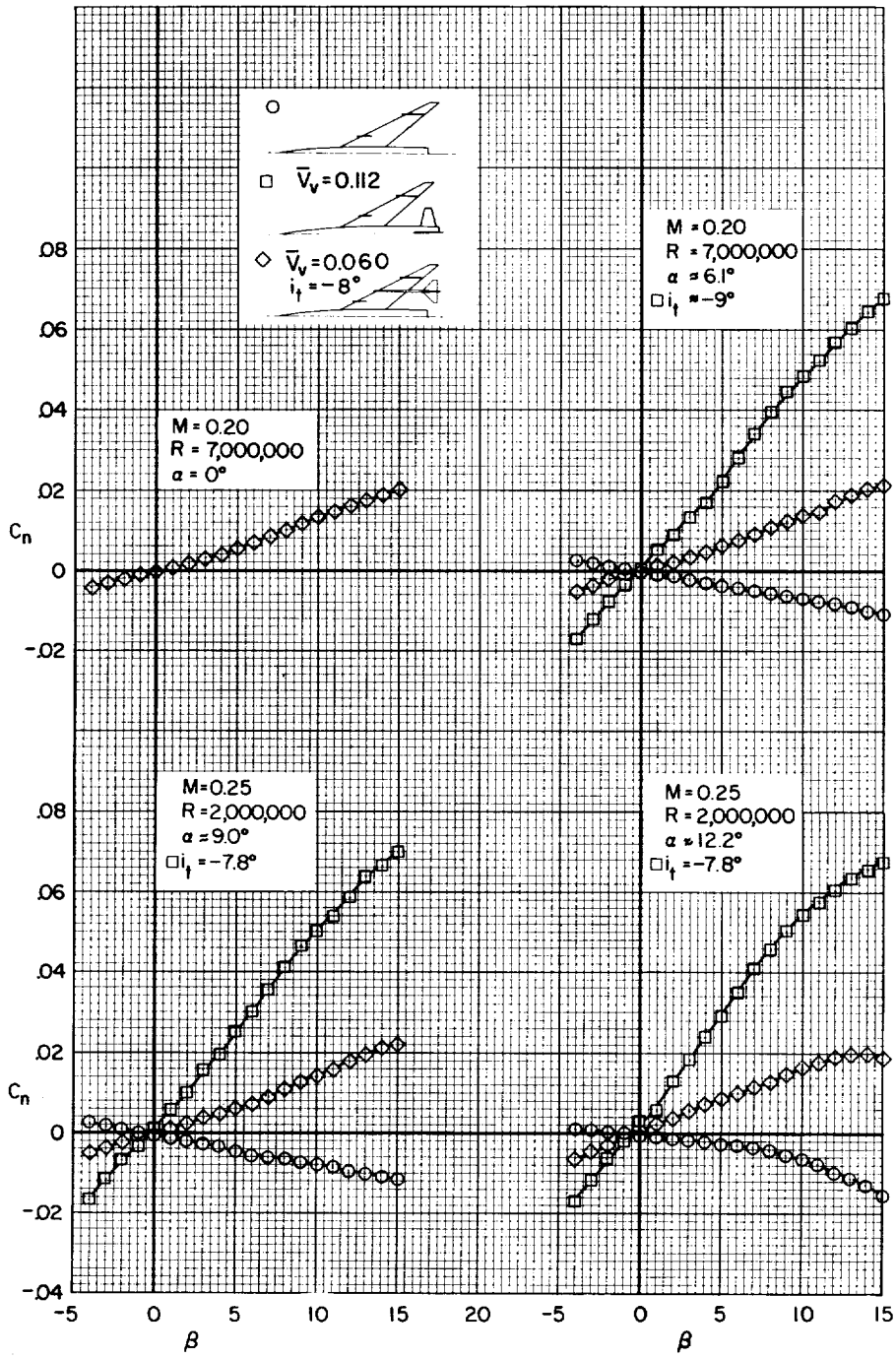

(a) M = 0.20 and 0.25

Figure 16.- The variation with angle of sideslip of the yawing-moment coefficient of the tail off, outboard, and conventional tail configurations.

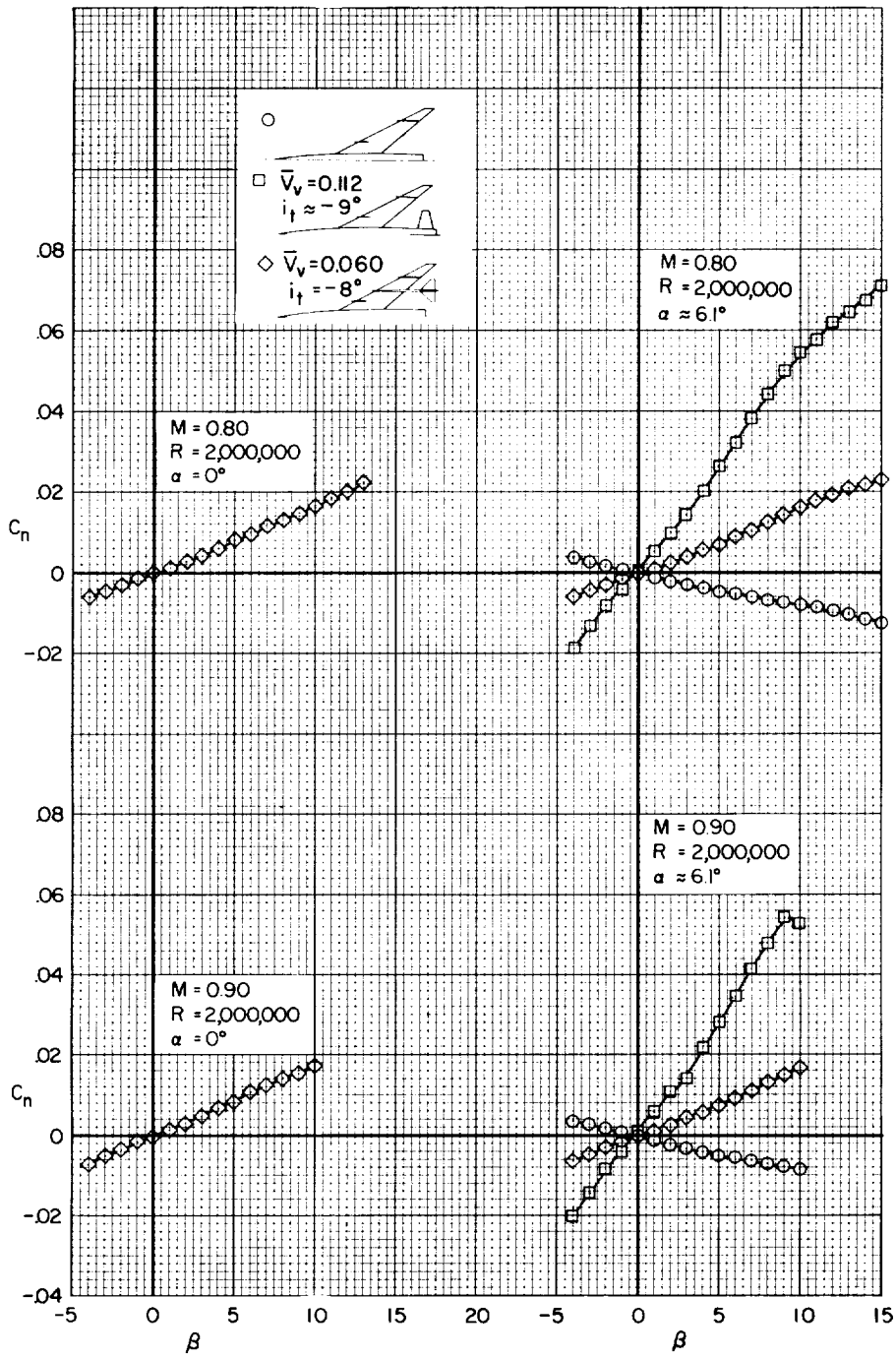

(b) M = 0.80 and 0.90

Figure 16.- Concluded.

[redacted]

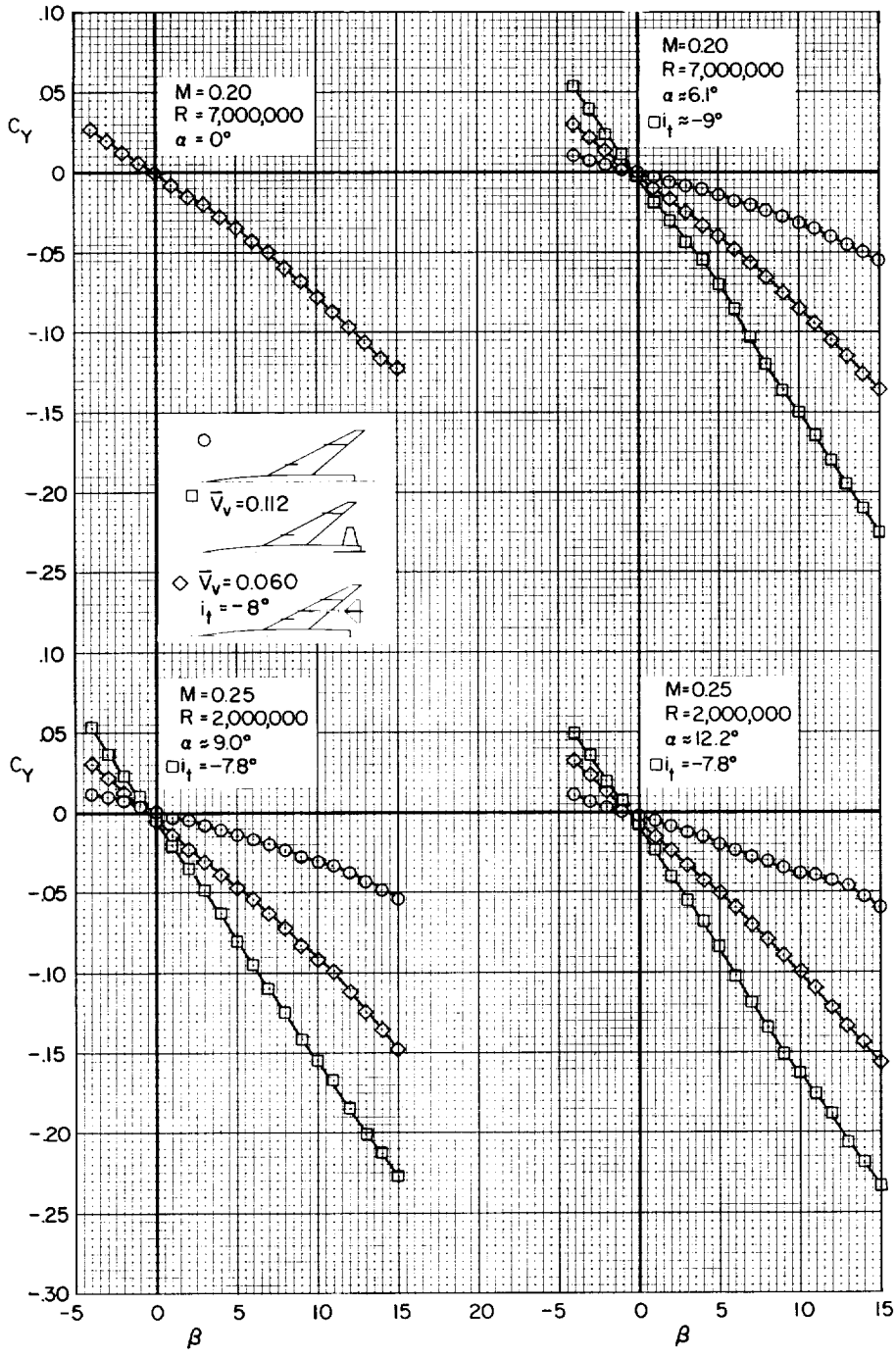

(a) M = 0.20 and 0.25

Figure 17.- The variation with angle of sideslip of the lateral-force coefficient of the tail off, outboard, and conventional tail configurations.

[redacted]

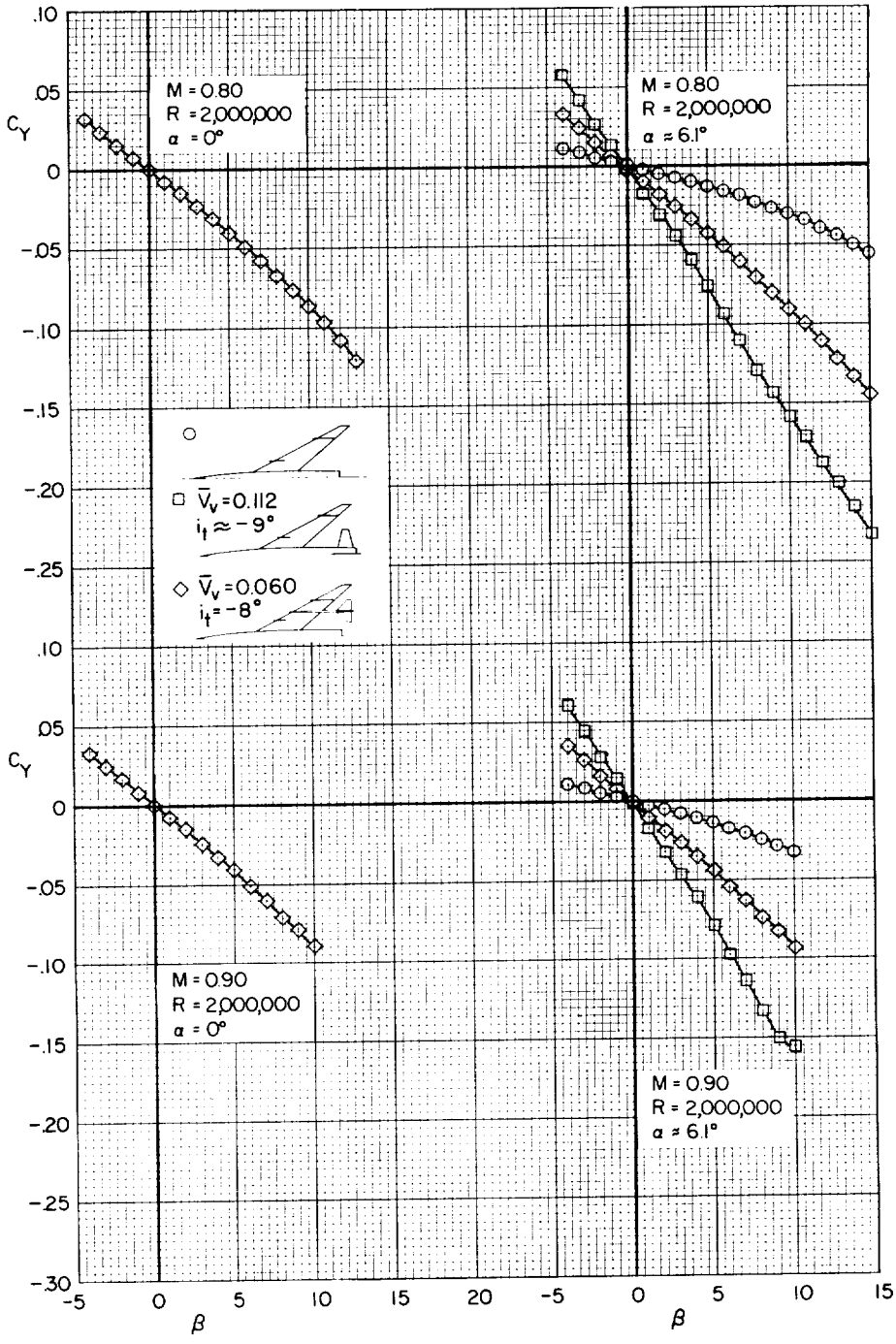

(b) M = 0.80 and 0.90

Figure 17.- Concluded.

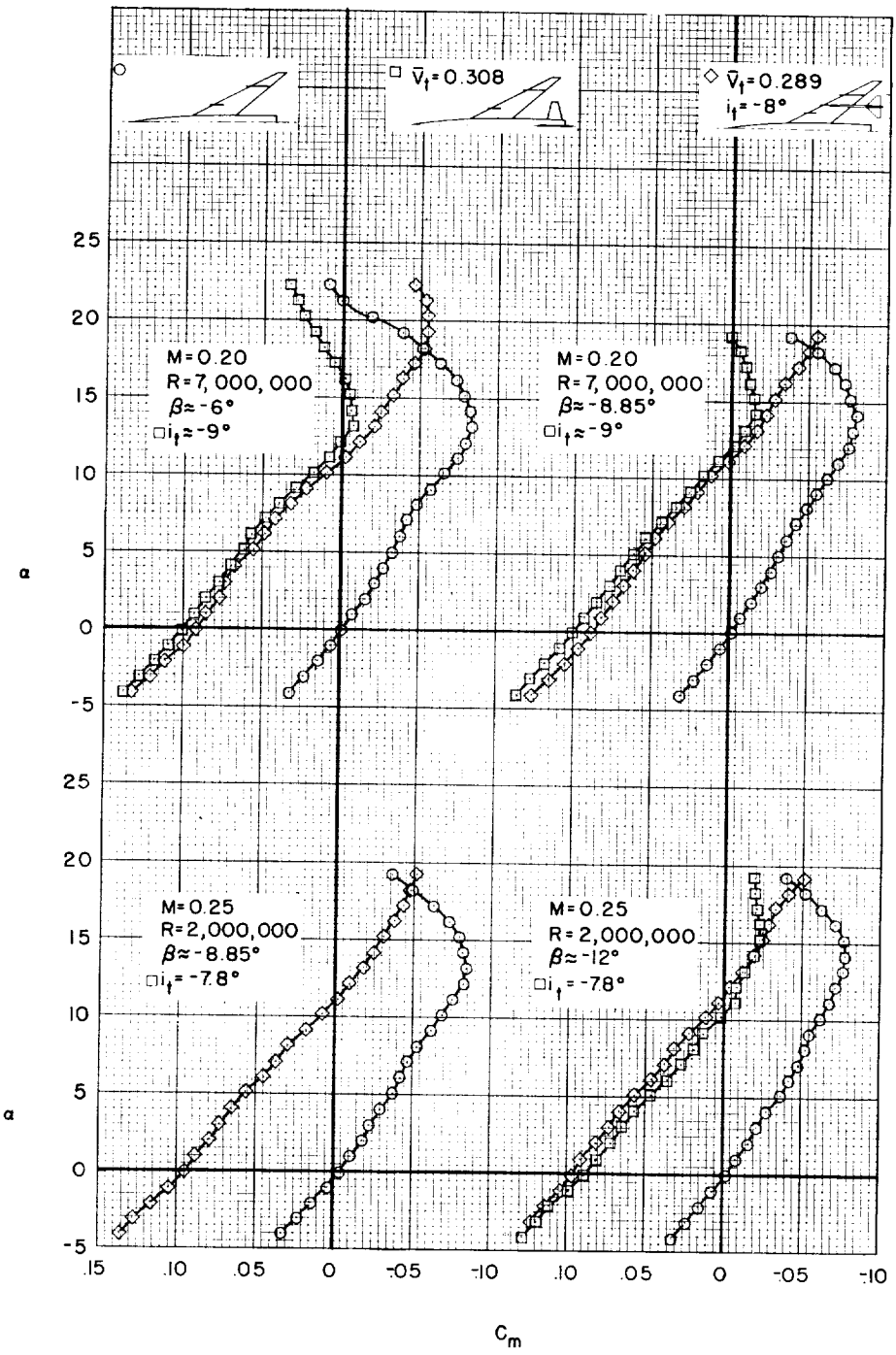

(a) M = 0.20 and 0.25

Figure 18.- The variation with angle of attack of the pitching-moment coefficient of the tail off, outboard, and conventional tail configurations.

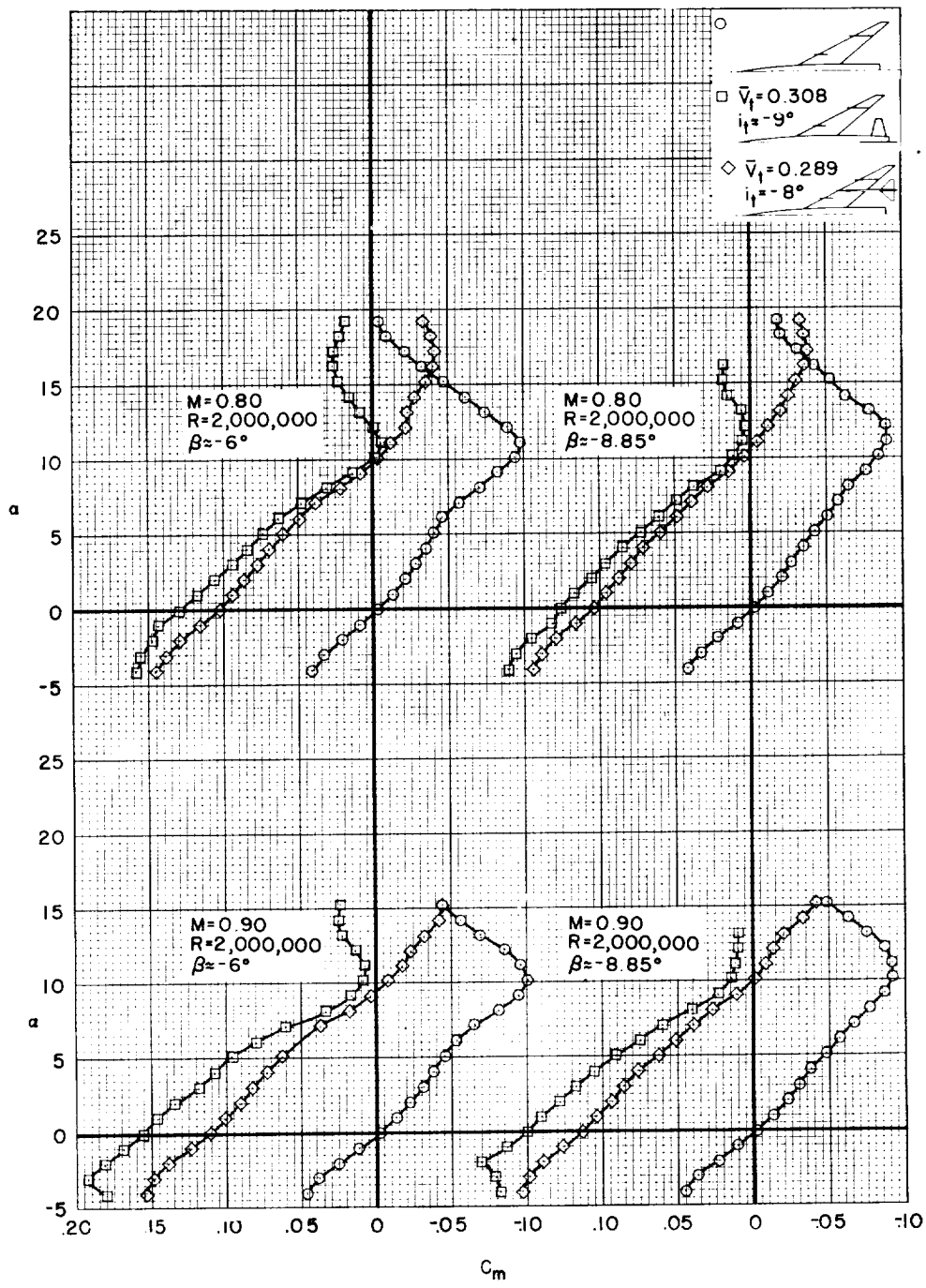

(b) M = 0.80 and 0.90

Figure 18.- Concluded.

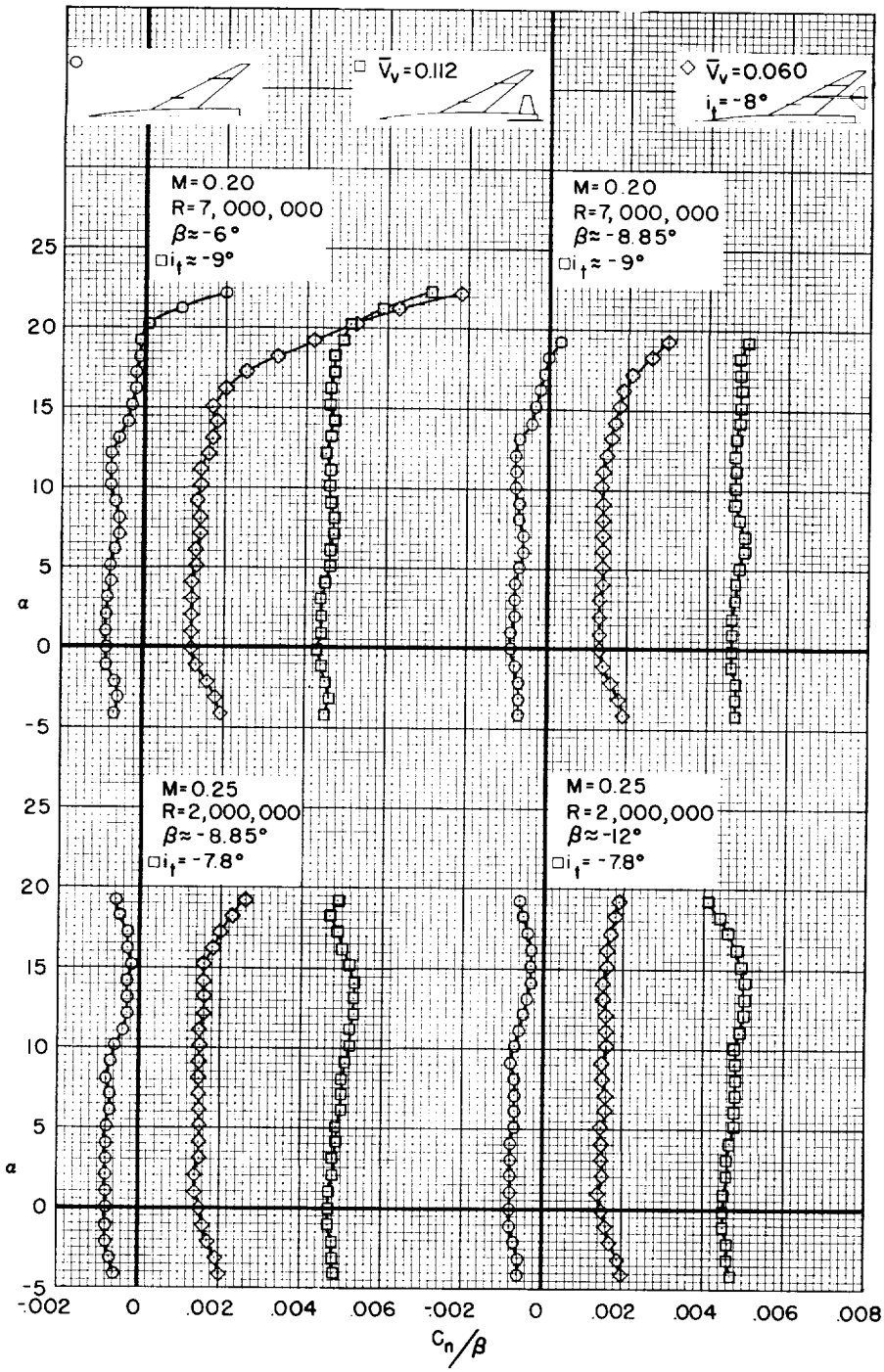

(a) M = 0.20 and 0.25

Figure 19.- The variation with angle of attack of C_n/β of the tail off, outboard, and conventional tail configurations.

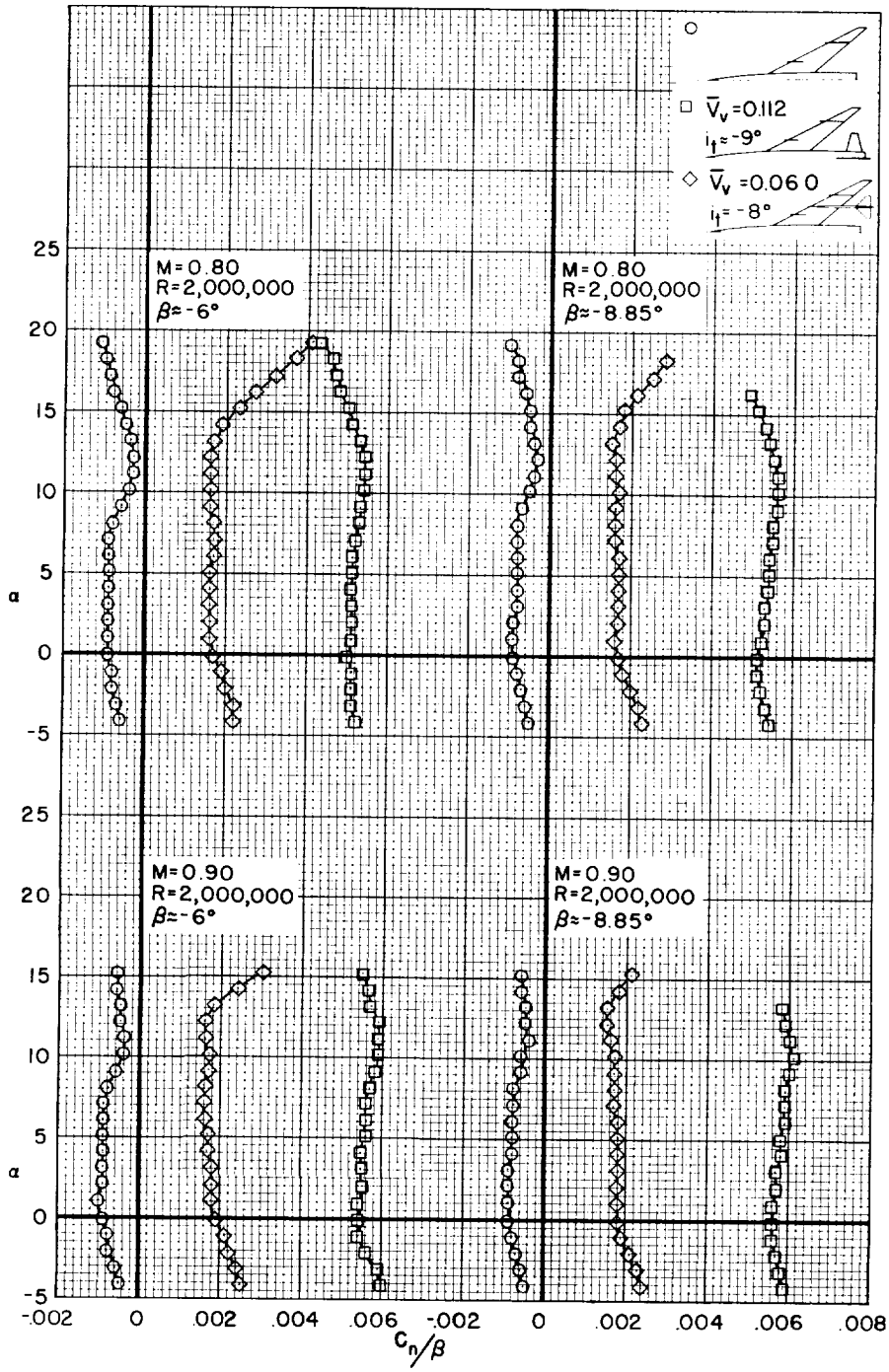

(b) M = 0.80 and 0.90

Figure 19.- Concluded.

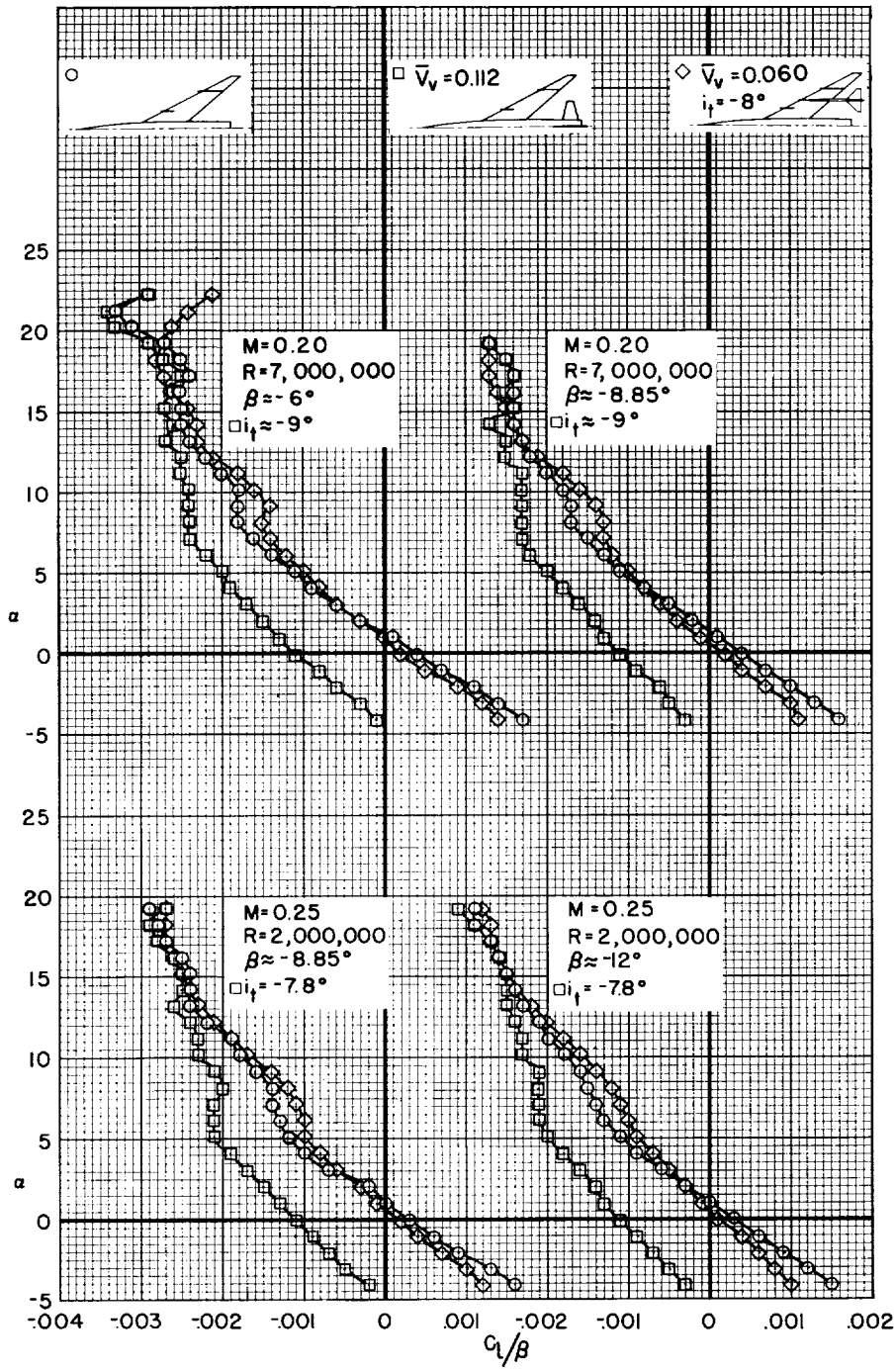

(a) M = 0.20 and 0.25

Figure 20.- The variation with angle of attack of C_l/β of the tail off, outboard, and conventional tail configurations.

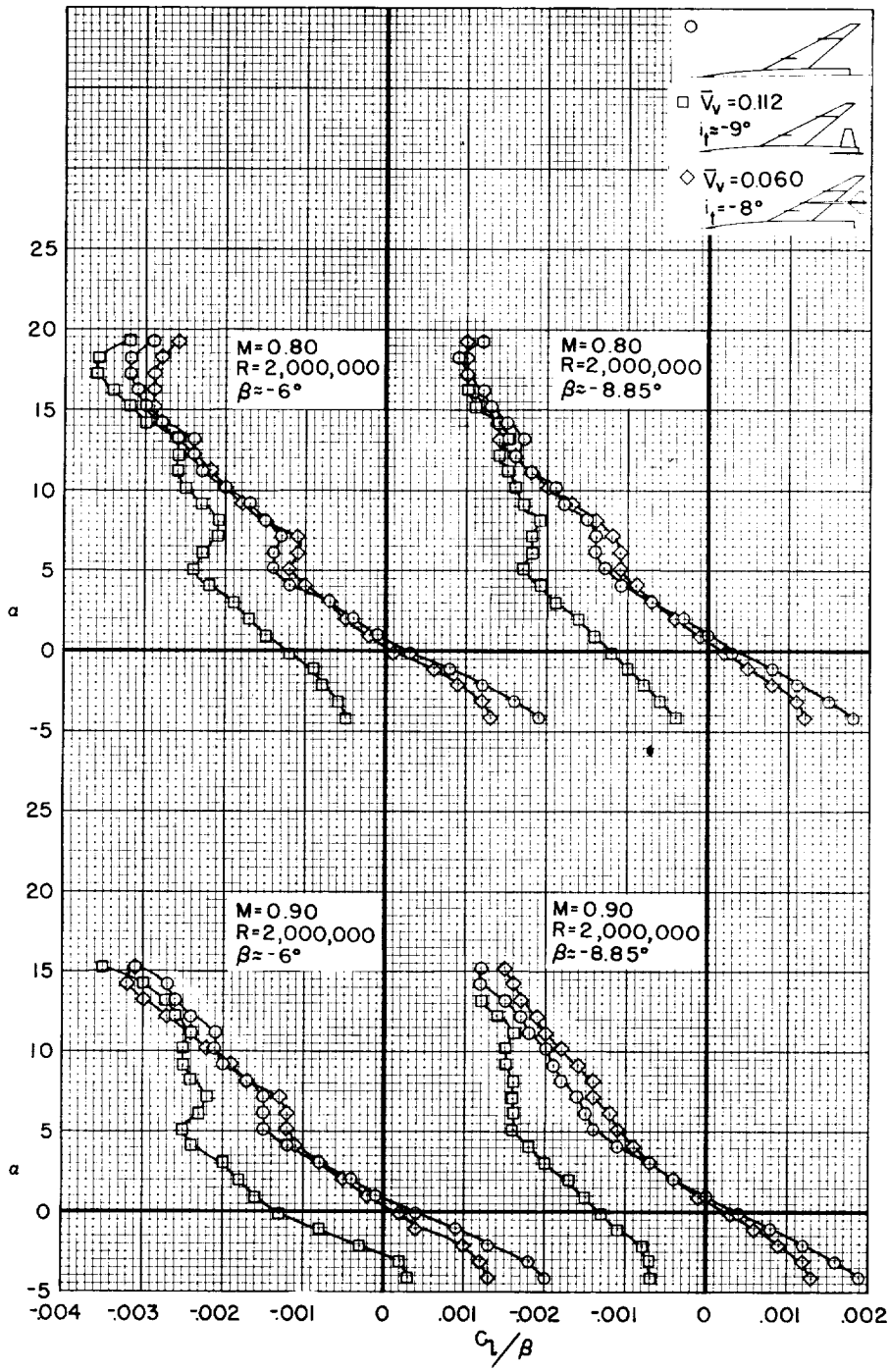

(b) M = 0.80 and 0.90

Figure 20.- Concluded.

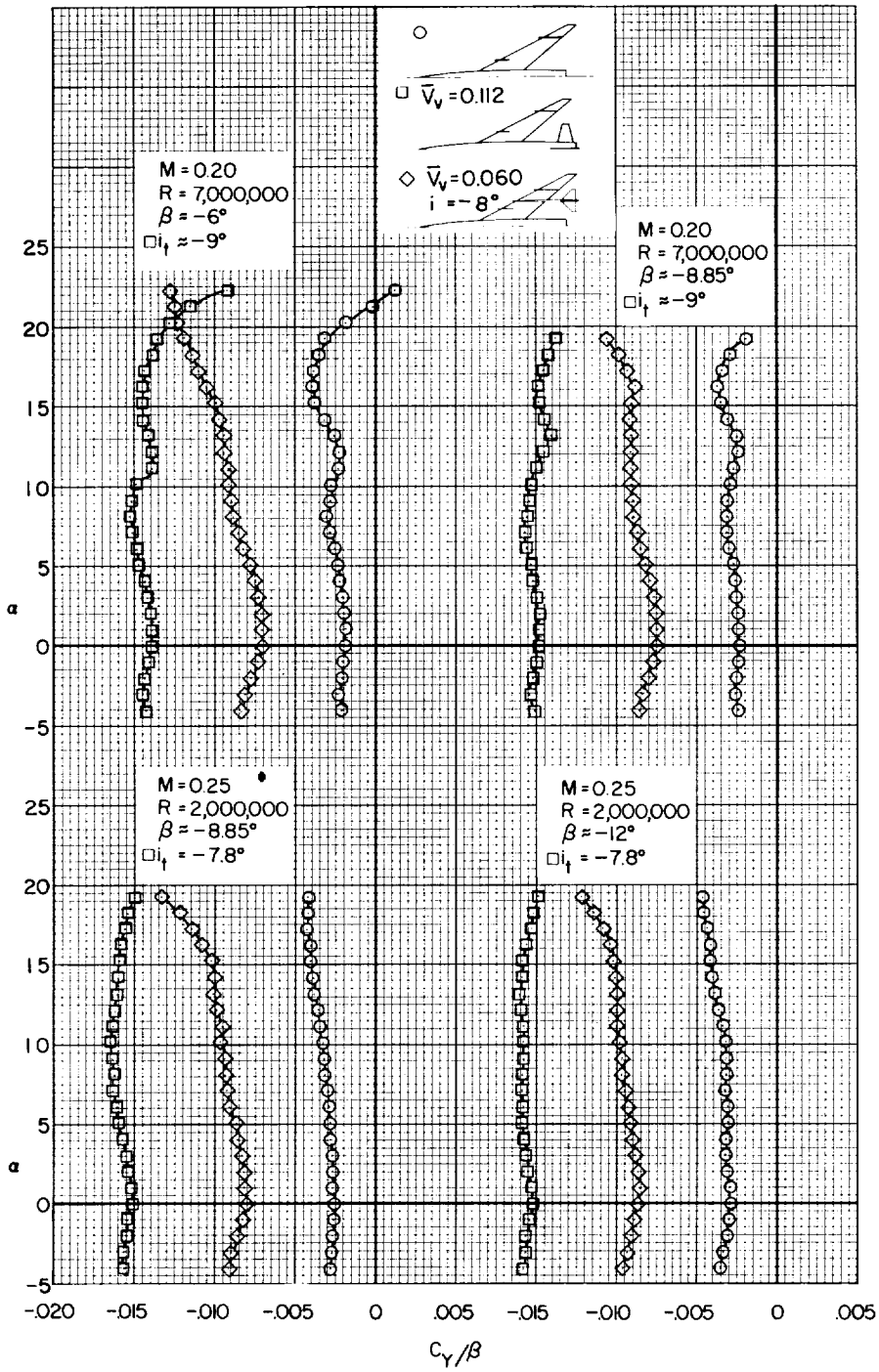

(a) M = 0.20 and 0.25

Figure 21.- The variation with angle of attack of C_Y/β of the tail off, outboard, and conventional tail configurations.

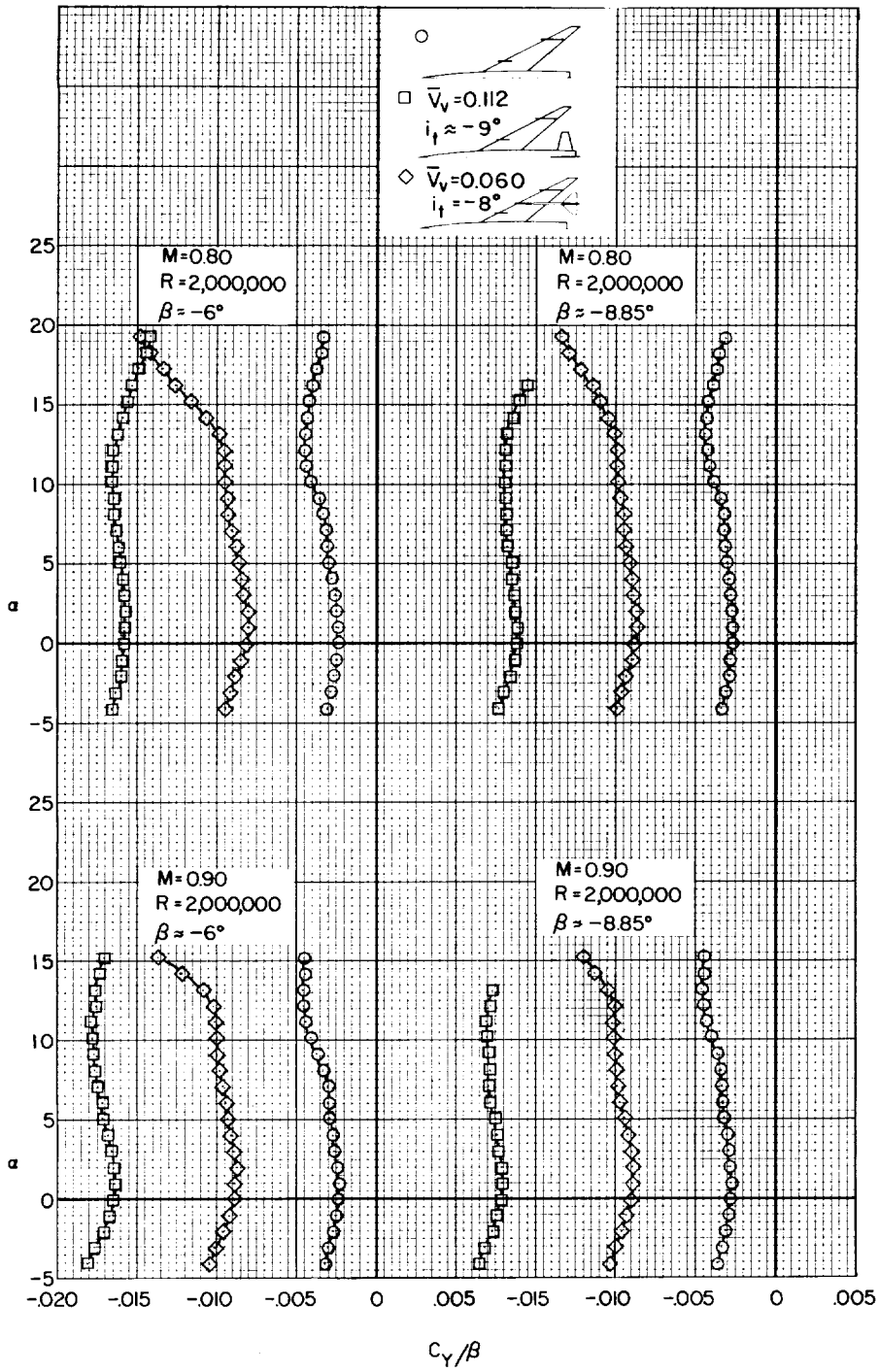

(b) M = 0.80 and 0.90

Figure 21.- Concluded.

NASA MEMO 3-3-59A
National Aeronautics and Space Administration.
SUBSONIC AERODYNAMIC CHARACTERISTICS OF AN AIRPLANE CONFIGURATION WITH A 63° SWEPT-BACK WING AND TWIN-BOOM TAILS. Howard F. Savage and George G. Edwards. March 1959. 57p. diagrs., photos., tabs.
(NASA MEMORANDUM 3-3-59A) CONFIDENTIAL
(Title, Unclassified)
The model tested had a wing of aspect ratio 3.5. Tail booms extending rearward from approximately the midsemispan of each wing panel supported independent tail assemblies. The longitudinal, lateral, and directional characteristics of this configuration were obtained at Mach numbers to 0.95 and the results are compared to those for the wing-fuselage combination with conventional fuselage-mounted tail. The effects of wing fences, an extended flap, and spoilers were also studied.

Copies obtainable from NASA, Washington

[redacted]

1. Flaps, Trailing-Edge - Complete Wings (1.2.2.3.1)
2. Tail-Wing-Fuselage Combinations - Airplanes (1.7.1.1.3)
3. Stability, Static (1.8.1.1)
4. Control, Longitudinal (1.8.2.1)
5. Control, Lateral (1.8.2.2)

I. Savage, Howard F.
II. Edwards, George G.
III. NASA MEMO 3-3-59A

NASA

[redacted]

NASA MEMO 3-3-59A
National Aeronautics and Space Administration.
SUBSONIC AERODYNAMIC CHARACTERISTICS OF AN AIRPLANE CONFIGURATION WITH A 63° SWEPT-BACK WING AND TWIN-BOOM TAILS. Howard F. Savage and George G. Edwards. March 1959. 57p. diagrs., photos., tabs.
(NASA MEMORANDUM 3-3-59A) CONFIDENTIAL
(Title, Unclassified)
The model tested had a wing of aspect ratio 3.5. Tail booms extending rearward from approximately the midsemispan of each wing panel supported independent tail assemblies. The longitudinal, lateral, and directional characteristics of this configuration were obtained at Mach numbers to 0.95 and the results are compared to those for the wing-fuselage combination with conventional fuselage-mounted tail. The effects of wing fences, an extended flap, and spoilers were also studied.

Copies obtainable from NASA, Washington

[redacted]

1. Flaps, Trailing-Edge - Complete Wings (1.2.2.3.1)
2. Tail-Wing-Fuselage Combinations - Airplanes (1.7.1.1.3)
3. Stability, Static (1.8.1.1)
4. Control, Longitudinal (1.8.2.1)
5. Control, Lateral (1.8.2.2)

I. Savage, Howard F.
II. Edwards, George G.
III. NASA MEMO 3-3-59A

NASA

[redacted]

[redacted]

CONFIDENTIAL

NASA MEMO 3-3-59A
National Aeronautics and Space Administration.
SUBSONIC AERODYNAMIC CHARACTERISTICS OF AN AIRPLANE CONFIGURATION WITH A 63° SWEPT-BACK WING AND TWIN-BOOM TAILS. Howard F. Savage and George G. Edwards. March 1959. 57p. diagrs., photos., tabs.
(NASA MEMORANDUM 3-3-59A) CONFIDENTIAL
(Title, Unclassified)
The model tested had a wing of aspect ratio 3.5. Tail booms extending rearward from approximately the midsemispan of each wing panel supported independent tail assemblies. The longitudinal, lateral, and directional characteristics of this configuration were obtained at Mach numbers to 0.95 and the results are compared to those for the wing-fuselage combination with conventional fuselage-mounted tail. The effects of wing fences, an extended flap, and spoilers were also studied.

Copies obtainable from NASA, Washington

1. Flaps, Trailing-Edge - Complete Wings (1.2.2.3.1)
2. Tail-Wing-Fuselage Combinations - Airplanes (1.7.1.1.3)
3. Stability, Static (1.8.1.1)
4. Control, Longitudinal (1.8.2.1)
5. Control, Lateral (1.8.2.2)

I. Savage, Howard F.
II. Edwards, George G.
III. NASA MEMO 3-3-59A

NASA

[redacted]

NASA MEMO 3-3-59A
National Aeronautics and Space Administration.
SUBSONIC AERODYNAMIC CHARACTERISTICS OF AN AIRPLANE CONFIGURATION WITH A 63° SWEPT-BACK WING AND TWIN-BOOM TAILS. Howard F. Savage and George G. Edwards. March 1959. 57p. diagrs., photos., tabs.
(NASA MEMORANDUM 3-3-59A) CONFIDENTIAL
(Title, Unclassified)
The model tested had a wing of aspect ratio 3.5. Tail booms extending rearward from approximately the midsemispan of each wing panel supported independent tail assemblies. The longitudinal, lateral, and directional characteristics of this configuration were obtained at Mach numbers to 0.95 and the results are compared to those for the wing-fuselage combination with conventional fuselage-mounted tail. The effects of wing fences, an extended flap, and spoilers were also studied.

Copies obtainable from NASA, Washington

[redacted]

1. Flaps, Trailing-Edge - Complete Wings (1.2.2.3.1)
2. Tail-Wing-Fuselage Combinations - Airplanes (1.7.1.1.3)
3. Stability, Static (1.8.1.1)
4. Control, Longitudinal (1.8.2.1)
5. Control, Lateral (1.8.2.2)

I. Savage, Howard F.
II. Edwards, George G.
III. NASA MEMO 3-3-59A

NASA

[redacted]